MODELING FREE RADICAL POLYMERIZATION:

CYCLIZATION AND CHAIN TRANSFER REACTIONS

by

İlke Uğur

B.S., Chemistry, Boğaziçi University, 2007

Submitted to the Institute for Graduate Studies in

Science and Engineering in partial fulfillment of

the requirements for the degree of

Master of Science

Graduate Program in Chemistry

Boğaziçi University

2009

MODELING FREE RADICAL POLYMERIZATION:

CYCLIZATION AND CHAIN TRANSFER REACTIONS

APPROVED BY :

Prof. Viktorya Aviyente ……………………….

(Thesis Supervisor)

Prof. Duygu Avcı ……………………….

Assoc. Prof. Nurcan Tüzün ……………………….

DATE OF APPROVAL: 08.06.2009

to my family...

ACKNOWLEDGEMENTS

ABSTRACT

MODELING FREE RADICAL POLYMERIZATION: CYCLIZATION AND CHAIN TRANSFER REACTIONS

In this study, the free radical polymerization of different unsaturated compounds is investigated.

In the first part entitled "Cyclopolymerization Reactions of Diallyl Monomers: Exploring Electronic and Steric Effects using DFT Reactivity Indices", the regioselectivity in the cyclopolymerization of diallyl monomers is investigated using DFT based reactivity indices. The experimentally observed mode of cyclization (exo versus endo) of eleven selected radicals involved in this process is reproduced by the computation of both activation energies, entropies, enthalpies, and Gibb's free energies for the 5- and 6-membered cyclization reactions. Next, a number of relevant DFT based reactivity indices such as non-spin polarized (f^0), spin polarized Fukui functions (f_{NN}^0), spin densities ρ_s, and dual descriptors ($f^{(2)}(r)$) were applied, in order to probe the role of the polar and stereoelectronic effects in this reaction. The dual descriptor has been found to reproduce best the experimental trends, confirming the important role of the stereo-electronic effects.

In the second part of this study entitled "Free Radical Polymerization of Acrylamide", the polymerization reaction of acrylamide is modeled in the presence of a series of thiophenols which act as chain transfer agents. Polyacrylamide, and copolymers of polyacrylamide have received considerable attention because they have reached large-scale industrial use. The process of chain transfer is used to control mostly the molecular weight, the structure and in some cases the functionality. The propagation rate analysis has showed that most accurate results can be obtained by using M05-2X/6-311++G(3df,2p) method. The correlation between the calculated trend of the chain transfer constants and the experimental results has been reproduced with the MPWB1K/6-311++G(3df,2p) methodology.

ÖZET

SERBEST RADİKAL POLİMERİZASYONUNUN MODELLENMESİ: SİKLİZASYON VE ZİNCİR TRANSFERİ TEPKİMELERİ

Bu çalışmada, farklı doymamış bileşiklerin serbest radikal polimerizasyonu incelendi.

"Dialil Monomerlerin Siklopolimerizasyon Tepkimeleri: Elektronik ve Sterik Etkilerin Yoğunluk Fonksiyonları Teorisi'ne (DFT) Dayanan Reaktivite Tanımlayıcıları Kullanılarak İncelenmesi" başlıklı birinci kısımda, Yoğunluk Fonksiyonları Teorisi'ne dayanan reaktivite tanımlayıcıları dialil monomerlerin siklopolimerizasyonundaki yerel seçiciliği tanımlamak üzere kullanıldı.

Seçilmiş onbir radikalin siklizasyon reaksiyonundaki deneysel olarak saptanmış yerel seçicikleri (exo ya da endo); eşik enerjileri, entropi, entalpi ve Gibbs serbest enerjileri hesaplanarak doğrulandı. Buna ek olarak, spin polarize edilmemiş (f^0), ve spin polarize edilmiş (f_{NN}^0) Fukui fonksiyonları, spin yoğunlukları (ρ_s), ve çift tanımlayıcıları ($f^{(2)}(r)$) gibi Yoğunluk Fonksiyonları Teorisi'ne (DFT) dayanan reaktivite tanımlayıcıları, polar ve stereo-electronik etkilerin bu reaksiyondaki rolünü anlamak üzere kullanıldılar. Stereo-electronik etkilerin önemli rolleri göz önünde bulundurulduğunda, çift tanımlayıcıların deneysel eğilimi en iyi yansıtan tanımlayıcılar oldukları saptanmıştır.

"Akrilamidin Serbest Radikal Polimerizayonu" isimli ikinci kısımda, zincir transfer reaksiyonu yapacak olan bir grup tiol monomerin varlığında akrilamidin polimerizasyon tepkimesi modellenerek incelendi. Poliakrilamid ve poliakrilamidin kopolimerleri, endüstrideki geniş kullanım alanları sebebiyle üzerinde birçok araştırma yapılan polimerlerdir. Zincir transferi tepkimesi ise polimerlerin moleküler ağırlığının, yapısının ve bazı durumlarda işlevselliğinin kontrol edildiği süreçlerdir. Yayılma hızı analizi, deneysel değerlere en yakın sayısal değerlerin M05-2X/6-311++G(3df,2p) yöntemi ile hesaplanabildiğini göstermiştir. Öte yandan, aynı analizde tiol monomerlerinin deneysel eğilimi en iyi MPWB1K/6-311++G(3df,2p) yöntemi ile hesaplanabilmiştir.

TABLE OF CONTENTS

LIST OF FIGURES

LIST OF TABLES

LIST OF SYMBOLS/ABBREVIATIONS

$E^{\ddagger}$	Electronic activation energy
E_c^{VWN}	Vosko-Wilk-Nusair correlation functional
E_x^{exact}	Exact exchange energy
$E_c[\rho]$	Correlation energy
$E_x[\rho]$	Exchange energy
$E_{\sigma\sigma*}$	Non-covalent contributions to the energy
ΔE_x^{B88}	Becke's gradient correction
ΔE_0	Relative electronic energy at 0 K
ΔE_{0+ZPE}	Sum of the change in electronic energy and zero point energy at 0 K
ΔE_{298}	Relative electronic energy at 298 K
$G^{\ddagger}$	Gibbs free energy of activation
ΔG_{298}	Relative Gibbs free energy at 298 K
ΔH_{298}	Relative enthalpy at 298 K
$\Delta H_{rxn.}$	Heat of reaction as electronic energy
$J[\rho]$	Coulomb energy
ΔS_{298}	Relative entropy at 298 K
$T[\rho]$	Kinetic energy of interacting electrons
$T_s[\rho]$	Kinetic energy of non-interacting electrons
U_x^{σ}	Exchange energy density
$V_{ee}[\rho]$	Interelectronic interaction energy
V_{KS}	Kohn-Sham potential
$v(r)$	External potential
$\rho(r)$	Electron density
ψ_i	Kohn-Sham orbitals
B3LYP	Becke-3-parameter Lee-Yang-Parr functional
DFT	Density functional theory
HF	Hartree-Fock theory
LDA	Local density approximation

k_i	Rate constant of initiation
k_p	Rate constant of propagation
k_t	Rate constant of termination
μ	Chemical potential
$f^0(r)$	Fukui function
$f_{NN}^{0}(r)$	Spin polarized Fukui function
ρ_s	Spin density
$f^{(2)}(r)$	Dual Descriptor

1. INTRODUCTION

1.1 Free Radical Polymerization

The polymerization of unsaturated monomers typically involves a chain reaction. In a typical chain polymerization, one act of initiation may lead to the polymerization of thousands of monomer molecules [1].

The characteristics of chain polymerization suggest that the active center responsible for the growth of the chain associated with a single polymer molecule through the addition of many monomer units [1].

The free radical polymerization process consists of a sequence of three steps: initiation, propagation, and termination. The initiation step is considered to proceed via two reactions. The first is the production of free radicals. The usual case is the homolytic dissociation of an initiator or a catalyst I to yield a pair of radicals $R \bullet$

$$I \xrightarrow{k_d} 2R \bullet \tag{1.1}$$

where k_d is the rate constant for the catalyst dissociation. The second part of the initiation involves the addition of this radical to the first monomer molecule to produce the chain initiating species $M_1 \bullet$

$$R_1 \bullet + M \xrightarrow{k_i} M_1 \bullet \tag{1.2}$$

where M represents a monomer molecule and k_i is the rate constant for the initiation step (Eq. 1.2). For the polymerization of $CH_2=CHY$, Eq. 1.2 takes the form

$$R \bullet + CH_2 = CHY \longrightarrow R - CH_2 - CHY \bullet \tag{1.3}$$

(The radical $R\bullet$ is often referred to as an initiator radical or a primary radical.)

The propagation consists of the growth of $M_1\bullet$ by the successive additions of large numbers (hundreds, and perhaps, thousands) of monomer molecules. Each addition creates a new radical which has the same identity as the previous one, except that it is larger by one monomer unit. The successive additions may be represented by

$$M_1\bullet + M \xrightarrow{k_p} M_2\bullet \tag{1.3}$$

$$M_2\bullet + M \xrightarrow{k_p} M_3\bullet \tag{1.4}$$

$$M_3\bullet + M \xrightarrow{k_p} M_4\bullet \tag{1.5}$$

or in general terms

$$M_n\bullet + M \xrightarrow{k_p} M_{n+1}\bullet \tag{1.6}$$

where k_p is the rate constant for propagation. Propagation with growth of the chain to high polymer proportions takes place very rapidly. The value of k_p for most monomers is in the range of 10^2-10^4 liter/mole-sec.

At some point, the propagation polymer chain stops growing and terminates. The termination with the annihilation of the radical centers occurs by bimolecular reaction between radicals. Two radicals react with each other by *combination* (*coupling* (k_{tc})),

$$\tag{1.7}$$
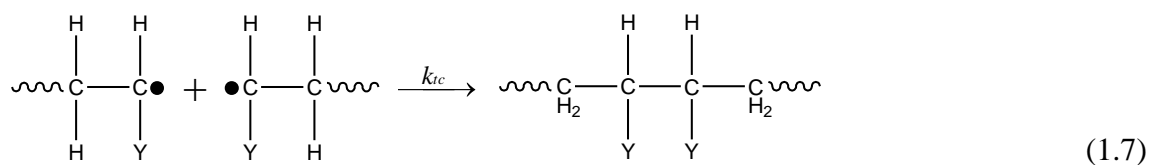
or, more rarely, by *disproportionation* in which a hydrogen radical that is *beta* to a radical center is transferred to another radical center (k_{td}). This results in the formation of two polymer molecules-one saturated and one unsaturated.

$$(1.8)$$
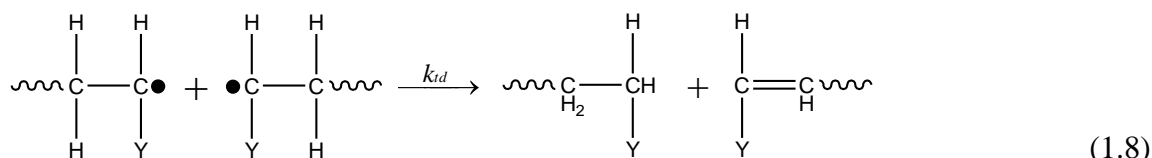
Termination can also occur by a combination of coupling and disproportionation. The two different modes of termination can be represented in general terms by

$$M_n \bullet + M_m \bullet \xrightarrow{\ k_{tc}\ } M_{n+m} \tag{1.9}$$

$$M_n \bullet + M_m \bullet \xrightarrow{\ k_{td}\ } M_n + M_m \tag{1.10}$$
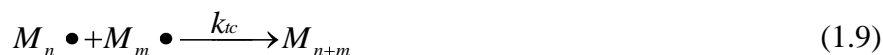
where k_{tc} and k_{td} are the rate constants for termination by coupling and disproportionation, respectively. One can also express the termination step by

$$M_n \bullet + M_m \bullet \xrightarrow{\ k_t\ } \text{ dead polymer} \tag{1.11}$$

where the particular mode of termination is not specified

$$k_t = k_{tc} + k_{td} \tag{1.12}$$

The term *dead polymer* signifies the cessation of growth for the propagating radical. The propagation reaction would proceed indefinitely until all the monomers in a reaction system are exhausted. Typical termination rate constants are in the range of 10^6-10^8 liter/mole-sec or orders of magnitude greater than the propagation rate constants. The much greater value of k_t (whether k_{tc} or k_{td}) compared to k_p does not prevent propagation because the radical species are present in very low concentrations.

1.2 Cyclopolymerization

Cyclopolymerization is one of the free radical polymerization methods which was proposed by Butler [2]. In this method, diallyl monomers polymerize via alternating intramolecular and intermolecular steps in chain growth reactions.

Cyclopolymerization mechanism has the same principle of free radical polymerization. In addition there are intermolecular competing reactions. The cyclopolymerization reaction mechanism of diallyl monomers can be considered mainly in 4 steps (Figure 1.1):

  i. Initiation
 ii. Cyclization
iii. Intermolecular Chain Propagation
 iv. Termination

The initiation of the diallyl molecule, creating a radical center, is followed by the intramolecular cyclization reaction. The intramolecular cyclization reactions give two possible products with two possible repeating units. The repeating cyclization units can be 5-membered-exo- or 6-membered-endo- cyclic structures, depending on the regioselectivity of the radical addition to the double bond. There are two possible propagation steps. One is the intermolecular propagation of the cyclized ring and the other one is the propagation of the uncyclized polymer chain. Then termination proceeds for both possible propagated polymers. (Figure 1.1)

Initiation
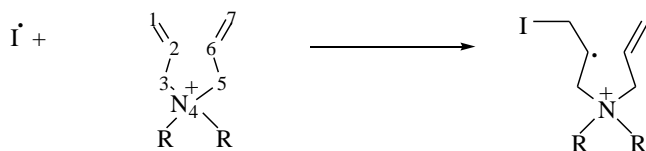
Cyclization
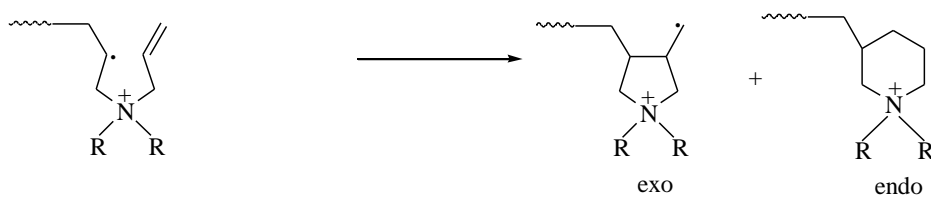
Intermolecular Propagation by the Ring
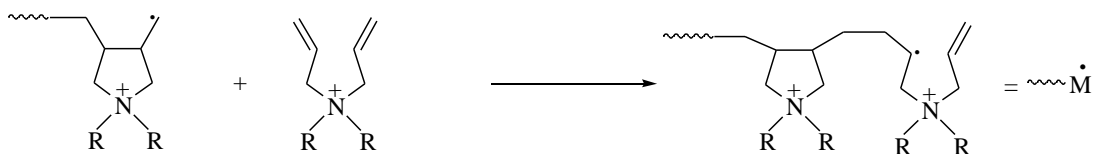
Intermolecular Propagation by the Uncyclized Polymer Chain
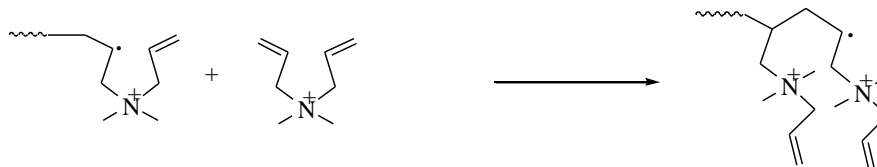
Chain Transfer

Termination
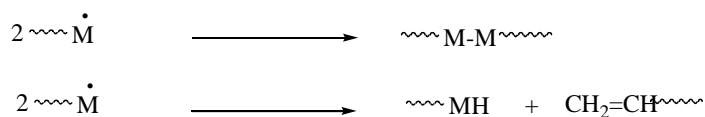
(I= Initiator, M=Monomer)

Figure 1.1. Cyclopolymerization mechanism and competing reactions

1.3. Free Radical Polymerization Kinetics

When the reaction kinetics is considered, the rate of initiation (υ_i) according to the initiation reaction may be given as

$$\upsilon_i = 2 f k_d [I] \tag{1.13}$$

where f, k_d and I denote the initiator efficiency, the rate constant for the decomposition of the initiator, and the concentration of the initiator, respectively. The initiator efficiency factor is used since all the generated free radicals are not able to initiate polymer growth. Sometimes recombination between radicals may take place. Initiator efficiency may take values between zero and one.

The rate of termination (υ_t) is a bimolecular process so that

$$\upsilon_t = 2 k_t [M^\bullet]^2 \tag{1.14}$$

where k_t and M stand for the termination rate constant and the concentration of the monomer respectively. The rate constant $2k_t$ is actually ($k_{tc} + k_{td}$).

According to the steady state approximation, the initiation is relatively small but continuous. The termination speeds up as the active radical concentration builds and the termination removes (kills) active radicals. Therefore it is an excellent approximation to assume that rate of initiation of radicals is equal to the rate of termination of radicals.

$$\upsilon_i = \upsilon_t \tag{1.15}$$

$$2 f k_d [I] = 2 k_t [M^\bullet]^2 \tag{1.16}$$

$$[M^\bullet] = \left(\frac{f k_d [I]}{k_t} \right)^{1/2} \tag{1.17}$$

Thus, rate of propagation (υ_p) may be given as

$$\upsilon_p = k_p[M][M^\bullet] = k_p[M]\left(\frac{fk_d[I]}{k_t}\right)^{1/2}$$ (1.18)

where k_p stands for the propagation rate constant. In the derivation of polymerization rate, the propagation (k_p) and termination (k_t) rate coefficients are assumed to be chain length and conversion independent [3, 4].

The overall homopolymerization rate constant, k, is based on the kinetic expression for homopolymerization [5]

$$R_p = k[I]^{1/2}[M]$$ (1.19)

Then, the expression for k is

$$k = \frac{k_p}{k_t^{1/2}}(fk_d)^{1/2}$$ (1.20)

2. AIM OF THE STUDY

This study consists of two parts. Each part mainly deals with the free radical polymerization of different unsaturated compounds.

The aim of the first part is to examine the regioselectivity in the cyclopolymerization of diallyl monomers by using quantum mechanical tools. Energetics and conceptual DFT based reactivity descriptors will be used to investigate the regioselectivity for the reaction mentioned above.

In the second part of this study, the free radical polymerization of the acrylamide monomer is investigated by molecular modelling. The geometrical features of the species involved in the free radical polymerization of acrylamide will be discussed. In addition, the kinetics of the propagation of acrylamide and the chain transfer reactions of a number of thiophenols along the polymerization of acrylamide will be examined.

3. THEORY

3.1 Density Functional Theory

Density Functional Theory (DFT) [6] is a quantum mechanical approach to the electronic structure of atoms and molecules based upon a theory presented by Kohn-Hohenberg proposed in 1964. [7, 8] Kohn-Hohenberg theorems state that all the ground-state properties of a system are functions of the charge density [7, 8].

The first theorem of DFT states that the electron density $\rho(r)$ determines the external potential $v(r)$, i.e. the potential due to the nuclei. The second theorem introduces the variational principle. Hence, the electron density can be computed variationally and the position of nuclei, energy, wave function and other related parameters can be calculated [6, 9].

The electron density is defined as:

$$\rho(r) = N \int ... \int |\Psi(x_1, x_2, ... x_n)|^2 \, dx_1 dx_2 ... dx_n \tag{3.1}$$

where x represents both spin and spatial coordinates of electrons.

The electronic energy can be expressed as a functional of the electron density:

$$E[\rho] = \int v(r) \rho(r) dr + T[\rho] + V_{ee}[\rho] \tag{3.2}$$

where $T[\rho]$ is the kinetic energy of the interacting electrons and $V_{ee}[\rho]$ is the interelectronic interaction energy. The electronic energy may be rewritten as

$$E[\rho] = \int v(r) \rho(r) dr + T_s[\rho] + J[\rho] + E_{xc}[\rho] \tag{3.3}$$

with $J[\rho]$ being the coulomb energy, $T_s[\rho]$ being the kinetic energy of the non-interacting electrons and $E_{xc}[\rho]$ being the exchange-correlation energy functional. The exchange-correlation functional is expressed as the sum of an exchange functional $E_x[\rho]$ and a correlation functional $E_c[\rho]$, although it contains also a kinetic energy term arising from the kinetic energy difference between the interacting and non-interacting electron systems. The kinetic energy term, being the measure of the freedom, and exchange-correlation energy, describing the change of opposite spin electrons (defining extra freedom to an electron), are the favorable energy contributions. The Coulomb energy term describes the unfavorable electron-electron repulsion energy and therefore disfavors the total electronic energy [10].

In Kohn-Sham density functional theory, a reference system of independent non-interacting electrons in a common, one-body potential V_{KS} yielding the same density as the real fully-interacting system is considered. More specifically, a set of independent reference orbitals ψ_i satisfying the following independent particle Schrödinger equation are imagined.

$$\left[-\frac{1}{2}\nabla^2 + V_{KS} \right]\psi_i = \varepsilon_i \psi_i \tag{3.4}$$

with the one-body potential V_{KS} defined as

$$V_{KS} = v(r) + \frac{\partial J[\rho]}{\partial \rho(r)} + \frac{\partial E_{xc}[\rho]}{\partial \rho(r)} \tag{3.5}$$

$$V_{KS} = v(r) + \frac{\rho(r')}{|r-r'|}dr' + v_{xc}(r) \tag{3.6}$$

where $v_{xc}(r)$ is the exchange-correlation potential. The independent orbitals ψ_i are known as Kohn-Sham orbitals and give the exact density by

$$\rho(r) = \sum_{i}^{N} |\psi_i|^2 \tag{3.7}$$

if the exact form of the exchange-correlation functional is known. However, the exact form of this functional is not known and approximate forms are developed starting with the local density approximation (LDA). This approximation gives the energy of a uniform electron gas, i. e. a large number of electrons uniformly spread out in a cube accompanied with a uniform distribution of the positive charge to make the system neutral. The energy expression is

$$E[\rho] = T_s[\rho] + \int \rho(r)v(r)dr + J[\rho] + E_{xc}[\rho] + E_b \qquad (3.8)$$

where E_b is the electrostatic energy of the positive background. Since the positive charge density is the negative of the electron density due to uniform distribution of particles, the energy expression is reduced to

$$E[\rho] = T_s[\rho] + E_{xc}[\rho] \qquad (3.9)$$

$$E[\rho] = T_s[\rho] + E_x[\rho] + E_c[\rho] \qquad (3.10)$$

The kinetic energy functional can be written as

$$T_s[\rho] = C_F \int \rho(r)^{5/3} dr \qquad (3.11)$$

where C_F is a constant equal to 2.8712. The exchange functional is given by

$$E_x[\rho] = -C_x \int \rho(r)^{4/3} dr \qquad (3.12)$$

with C_x being a constant equal to 0.7386. The correlation energy, $E_c[\rho]$, for a homogeneous electron gas comes from the parametrization of the results of a set of quantum Monte Carlo calculations.

The LDA method underestimates the exchange energy by about 10 per cent and does not have the correct asymptotic behavior. The exact asymptotic behavior of the exchange energy density of any finite many-electron system is given by

$$\lim_{x \to \infty} U_x^{\sigma} = -\frac{1}{r}$$

(3.13)

U_x^{σ} being related to $E_x[\rho]$ by

$$E_x \big[\big] = -\frac{1}{2} \sum_{\sigma} \int \rho_{\sigma} U_x^{\sigma} dr$$

(3.14)

A gradient-corrected functional is proposed by Becke

$$E_x = E_x^{LDA} - \beta \sum_{\sigma} \int \rho_{\sigma}^{4/3} \frac{x_{\sigma}^2}{1 + 6\beta x_{\sigma} \sinh^{-1} x_{\sigma}} dr$$

(3.15)

where σ denotes the electron spin, $x_{\sigma} = \frac{|\nabla \rho_{\sigma}|}{\rho_{\sigma}^{4/3}}$ and β is an empirical constant ($\beta = 0.0042$). This functional is known as Becke88 (B88) functional [11].

The adiabatic connection formula connects the non-interacting Kohn-Sham reference system ($\lambda = 0$) to the fully-interacting real system ($\lambda = 1$) and is given by

$$E_{xc} = \int_0^1 U_{xc}^{\lambda} d\lambda$$

(3.16)

where λ is the interelectronic coupling-strength parameter and U_{xc}^{λ} is the potential energy of exchange-correlation at intermediate coupling strength. The adiabatic connection formula can be approximated by

$$E_{xc} = \frac{1}{2} E_x^{exact} + \frac{1}{2} U_{xc}^{LDA}$$

(3.17)

since $U_{xc}^0 = E_x^{exact}$, the exact exchange energy of the Slater determinant of the Kohn-Sham orbitals, and $U_{xc}^1 = U_{xc}^{LDA}$ [12].

The closed shell Lee-Yang-Parr (LYP) correlation functional [13] is given by

$$E_c = -a \int \frac{1}{1+d\rho^{-\frac{1}{3}}} \left\{ \rho + b\rho^{-\frac{2}{3}} \left[C_F \rho^{\frac{5}{3}} - 2t_w + (\frac{1}{9}t_w + \frac{1}{18}\nabla^2\rho) \right] e^{-c\rho^{-\frac{1}{3}}} \right\} dr \quad (3.18)$$

where

$$t_w = \frac{1}{8} \frac{|\nabla\rho|^2}{\rho} - \frac{1}{8}\nabla^2\rho \quad (3.19)$$

The mixing of LDA, B88, E_x^{exact} and the gradient-corrected correlation functionals to give the hybrid functionals [14] involves three parameters.

$$E_{xc} = E_{xc}^{LDA} + a_0 \left(E_x^{exact} - E_x^{LDA} \right) + a_x \Delta E_x^{B88} + a_c \Delta E_c^{non-local} \quad (3.20)$$

where ΔE_x^{B88} is the Becke's gradient correction to the exchange functional. In the B3LYP functional, the gradient-correction ($\Delta E_c^{non-local}$) to the correlation functional is included in LYP. However, LYP contains also a local correlation term which must be subtracted to yield the correction term only.

$$\Delta E_c^{non-local} = E_c^{LYP} - E_c^{VWN} \quad (3.21)$$

where E_c^{VWN} is the Vosko-Wilk-Nusair correlation functional, a parameterized form of the LDA correlation energy based on Monte Carlo calculations. The empirical coefficients are a_0=0.20, a_x=0.72 and a_c=0.81 [15].

3.2. Reactivity Descriptors

The concepts of chemical hardness (η) and its inverse, the chemical softness (S) were introduced by Pearson [16] in the early sixties when comparing the stabilities of reaction products of Lewis acid-base reactions. On the basis of these data, a classification of Lewis acids and bases as hard and soft were presented in terms of polarizability, easiness to oxidize, etc. Pearson then formulated his famous hard and soft acids and bases (HSAB) principle stating that the hard acids prefer to interact with hard bases and similarly for soft acids and soft bases [16-18].

3.2.1. Global Descriptors

The chemical potential (μ) is a global property that determines the extent of a reaction.

$$\mu = -\chi = \left(\frac{\partial E}{\partial N} \right)_{v(\mathrm{r})} \approx -\frac{I + A}{2} \tag{3.22}$$

where E is the total energy, N is the number of electrons of the chemical species and μ is the chemical potential, which is identified as the negative of the electronegativity (χ):

$$-\chi = \mu \tag{3.23}$$

Parr and Pearson first provided the analytical definition of global hardness of any chemical species as

$$\eta = \left(\frac{\partial^2 E}{\partial N^2} \right)_{v(r)} = \left(\frac{\partial \mu}{\partial N} \right)_{v(r)} \tag{3.24}$$

The corresponding global softness is expressed as

$$S = \frac{1}{2\eta} = \left(\frac{\partial^2 N}{\partial E^2} \right)_{v(r)} = \left(\frac{\partial N}{\partial \mu} \right)_{v(r)} \tag{3.25}$$

By applying the finite difference approximation to equation 3.23, the operational definition of η and S can be obtained as

$$\eta = \frac{IP - EA}{2} \qquad (3.26)$$

$$S = \frac{1}{IP - EA} \qquad (3.27)$$

where IP and EA are the ionization potential and electron affinity of the chemical species.

According to Koopman's theorem, the ionization energy is simply the orbital energy of the HOMO, with change in sign. For spin paired molecules, the electron affinity is the negative of the orbital energy of the LUMO.

3.2.2. Local Descriptors

Local softness $s(r)$ describes local perturbation in terms of electron density ($\rho(r)$) with respect to a global change in chemical potential (μ),

$$s(r) = \left(\frac{\partial \rho(r)}{\partial \mu} \right)_{v(r)} \qquad (3.28)$$

so that

$$\int s(r) dr = S \qquad (3.29)$$

Combining Equations 3.25 and 3.28, s(r) can be written as

$$s(r) = \left(\frac{\partial \rho(r)}{\partial N} \right)_{v(r)} \left(\frac{\partial N}{\partial \mu} \right)_{v(r)} = f(r)S = \left(\frac{\partial \mu}{\partial v(r)} \right)_{N} S \qquad (3.30)$$

where $f(r)$ is defined as the Fukui function. Local softness contains the same information as Fukui functions (Eqn. 3.30) plus additional information about the total molecular softness. Therefore either the Fukui function or local softness can be used in studies of intramolecular reactivity sequences (i.e., relative site reactivity in a molecule). But only s(r) (not $f(r)$) should be a better descriptor of the global reactivity with respect to a reaction partner with a given hardness (or softness), as stated in the HSAB principle.

The Fukui function can be computed either for a nucleophilic ($f^+(\mathbf{r})$), an electrophilic ($f(\mathbf{r})$) or a radical attack ($f^0(\mathbf{r})$): [19]

$$f^+(r) = \left(\frac{\delta\rho(r)}{\delta N}\right)^+_{\vartheta(r)} \approx \rho_{N+1}(r) - \rho_N(r) \qquad (3.31)$$

$$f^+(r) = \left(\frac{\delta\rho(r)}{\delta N}\right)^-_{\vartheta(r)} \approx \rho_N(r) - \rho_{N-1}(r) \qquad (3.32)$$

$$f^0(r) = \frac{f^+(r)+f^-(r)}{2} \qquad (3.33)$$

using the Finite Differences Approximation (FDA), where $\rho_N(\mathbf{r})$, $\rho_{N+1}(\mathbf{r})$ and $\rho_{N-1}(\mathbf{r})$ are the densities of the N, $N+1$ and $N-1$ electron system, computed at the geometry of the N-electron system.

A more convenient way of calculating the f(r) functions is to use the condensed Fukui functions obtained from the previous equations, when integrated over the kth atomic region for the nucleophilic, electrophilic and radical attacks, respectively.

$$f^+(r) = q_k(N+1) - q_k(N) \qquad (3.34)$$

$$f^-(r) = q_k(N) - q_k(N-1) \qquad (3.35)$$

$$f^0(r) = {}^1\!/_2 \left[q_k \left(N + 1 \right) - q_k \left(N - 1 \right) \right] \qquad (3.36)$$

Here q_k is the electronic population of atom k in the molecule under consideration. It is known that these descriptors are generally used to probe the regio-selective nature of a reaction.

3.3. Continuum Solvation Models

In continuum solvation models [20, 21], the solvent is represented as a uniformpolarizable medium characterized by its static dielectric constant ε. In basic continuum solvation models, the solute is described at a homogenous quantum mechanical (QM) level and the solute-solvent interactions are limited to those of electrostatic terms. The total solvation free energy may be written as

$$\Delta G_{solvation} = \Delta G_{cavity} + \Delta G_{dispersion} + \Delta G_{electrostatic} \qquad (3.37)$$

In this representation, ΔG_{cavity} is the energetic cost of creating a cavity in the medium producing a destabilization effect. Dispersion interactions between solvent and solute add stabilization to solvation free energy term are expressed as $\Delta G_{dispersion}$. The latter electrostatic term, $\Delta G_{electrostatic}$, has a stabilization effect and furthermore it appears to be responsible for the main structural changes of the solute**.**

The solute charge distribution within the cavity induces a polarization of the surrounding medium, which in turn induces an electric field within the cavity called the *reaction field*. This field then interacts with solute charges, providing additional stabilization. The effect of the reaction field may be modeled by an appropriately distributed set of induced polarization charges on the surface S of the dielectric. The charge density on the surface of the cavity ,$\sigma(\vec{r}S)$, is given by the standard electrostatics in terms of the dielectric constant, ε, and the electric field perpendicular to the surface, $\vec{F}$, generated by the charge distribution within the cavity

$$4\pi\varepsilon\sigma(\vec{r}S) = (\varepsilon - 1) \, \vec{F} \, (\vec{r}S) \qquad (3.38)$$

Once $\sigma(\vec{r}S)$ is determined, the associated potential is added as an extra term to the Hamiltonian operator

$$H = H_o + V_\sigma \tag{3.39}$$

$$V_\sigma(\vec{r}) = \int \frac{\sigma(\vec{r}S)}{|\vec{r}-\vec{r}_s|} d\vec{r}_s \tag{3.40}$$

The potential from the surface charge $V\sigma$ is given by the molecular charge distribution but also enters the Hamiltonian and thus influences the molecular wave function, the procedure is therefore iterative.

In the Polarized Continuum solvation Models (PCM), the solute is embedded in a cavity defined by a set of spheres centered on atoms (sometimes only on heavy atoms), having radii defined by the van der Waals radius of the atoms multiplied by a predefined factor (usually 1.2). The cavity surface is then subdivided into small domains (called tesserae), where the polarization charges are placed. Among the many solutions to the electrostatic problem is the Integrated Equation Formalism (IEF) originally formulated by Cancés and Menucci [22-24]. The IEF-PCM method is a recent development in the polarized continuum models and has been utilized for solvent calculations in this study. It is based on the use of operators largely exploited in the theory of integral equations. The concept of cavity and of its tessellation is conserved. The IEF formalism is in fact able to treat a larger class of electrostatic problems.

4. CYCLOPOLYMERIZATION REACTIONS OF DIALLYL MONOMERS: EXPLORING ELECTRONIC AND STERIC EFFECTS USING DFT REACTIVITY INDICES

4.1 Introduction

Early in history it has been established that nonconjugated dienes, when subjected to addition polymerization, form either linear polymers containing unreacted double bonds or, more likely, crosslinked polymers [2]. On the other hand, allyl monomers are also known as poor monomers to yield high molecular weight polymers via polymerization reactions [20]. The abstraction of the reactive allylic hydrogen of the monomer causes chain transfer reactions which yield decreased molecular weight polymers [23, 24]. During a research carried out between 1949 to 1957 it was found that several polymers produced from diallyl quaternary ammonium salts had high molecular weights and were not crosslinked [2]. This fact shows that although allyl compounds are not good monomers for polymerization, their difunctional analogues, nonconjugated dienes, can be polymerized through cyclopolymerization (Scheme 1). Butler's discovery of polymerizations of diallyl compounds, later named "cyclopolymerizations", made it possible to synthesize high molecular weight water-soluble polymers from diallyl monomers [25, 26]. Because of their properties, these cyclopolymers are suitable for a wide range of industrial applications such as paper manufacturing, retention and drainage agents, wet strength additives, in water treatment industry, and mining industry [27] .
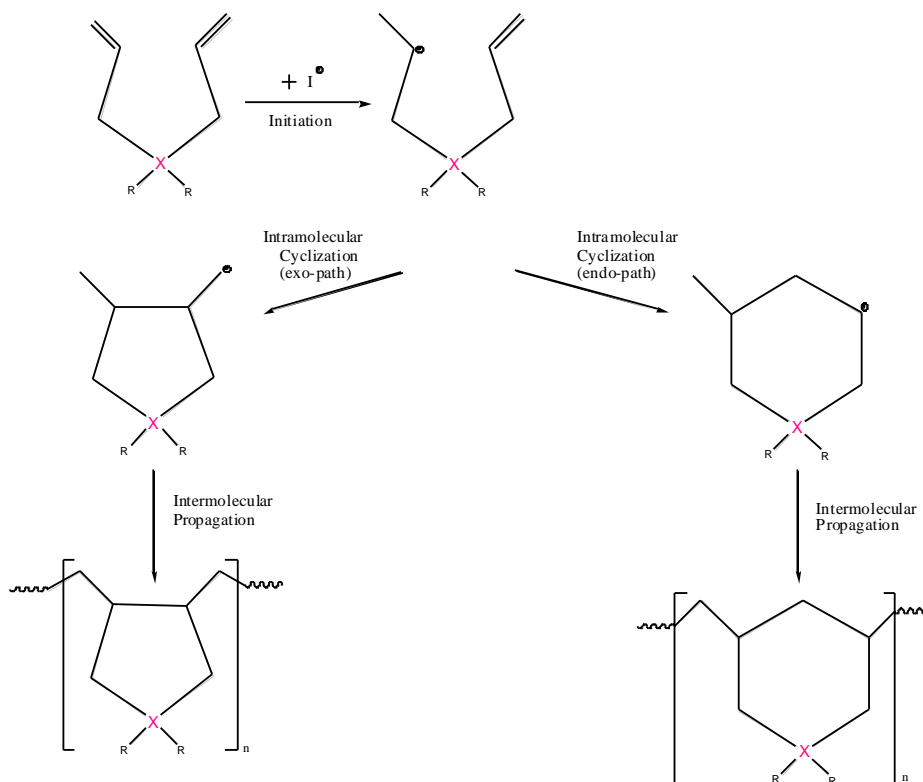
Figure 4.1. Cyclopolymerization reactions of diallyl monomers considered in this study.

(X=N,O; R=H, CH3, lone pair, I=Initiator)

The cyclopolymerization reaction of the diallyl monomers starts with the initiation of the diallyl molecule, creating a radical center, which is followed by the cyclization reaction that is the focus of this contribution. The intramolecular cyclization reactions give two possible products with two possible repeating units. The repeating cyclization units can be 5-membered-exo- or 6-membered-endo- cyclic structures, depending on the regioselectivity of the radical addition to the double bond (Figure 4.1). Next, the cyclized radical reacts with another monomer and the polymerization proceeds; this is called intermolecular propagation as depicted in Figure 4.1.
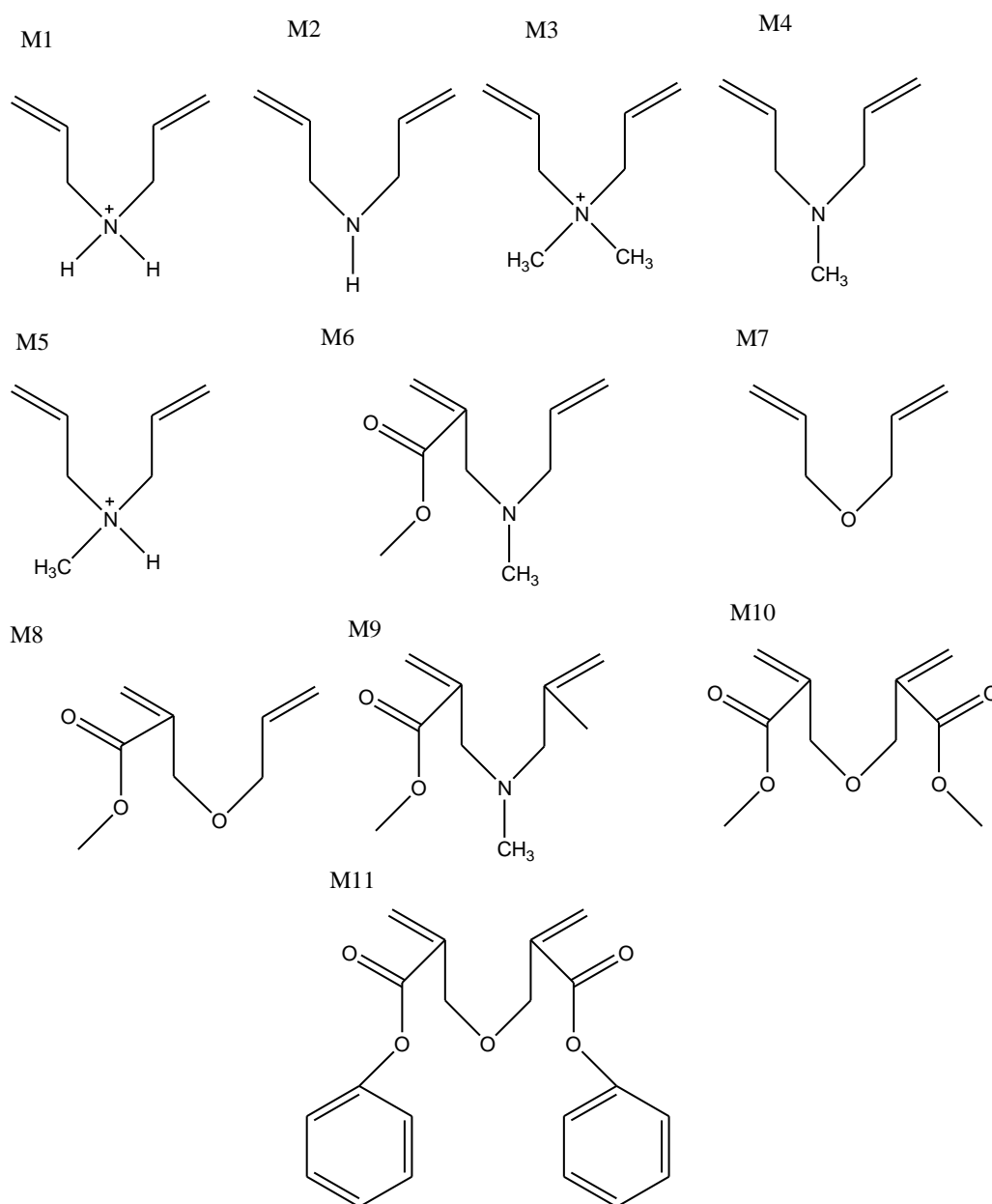
Figure 4.2. Reactive conformation structures of the different diallyl monomers investigated in the present work.

In this study, the regioselectivity in this first radical cyclization step of the cyclopolymerization reactions of the diallyl compounds, yielding 5-membered or 6-membered cyclic monomers, will be investigated using DFT reactivity indices (Figure 4.2). Monomers M1 to M8, (M1= *N*-methyl-*N*,*N*-diallylammonium, M2= *N*,*N*-diallylamine, M3=*N*,*N*-dimethyl-*N*,*N*-diallylamonium, M4=*N*methyl-*N*,*N*-diallylamine, M5= *N*,*N*-dimethyl-*N*,*N*-diallylammonium, M6= *N*-methyl-*N*-allyl-2-(methoxycarbonyl)allylamine,

M7=diallyl ether, M8= methyl α-(allyloxymethyl)acrylate) are known to cyclopolymerize to yield polymers with 5-membered ring units. M9, M10 and M11 (M9= *N*-methyl-*N*-methallyl-2-(methoxycarbonyl)allylamine, M10= methyl α –hydroxymethlacrylate, M11= α-(2-phenylallyloxy)methylstyrene) are known to cyclopolymerize to yield polymers with 6-membered ring units. In our earlier studies, the exo vs endo preferences of the models were rationalized based on steric, stereo-electronic, polar, and entropic effects [28-31]. The calculated thermochemical parameters such as activation entropies, enthalpies and free energies for the cyclization reactions have been found to be in agreement with experiment [28-31]. An NBO analysis on diallyl ether and methyl α-[(allyloxy)methyl]acrylate has indicated that the regioselectivity may be sensitive to hyperconjugative interactions [29].

In the present contribution, various descriptors, defined within the framework of density functional theory (DFT), are used to explain the regioselectivity of the radical cyclizations preceding the intermolecular propagation step in the cyclopolymerization reactions. The transition states and the activation barriers for both the exo and the endo modes of the cyclization for a number of diallyl radicals, depicted in Figure 4.3, are determined. An alternative and recently introduced energy decomposition of the activation barriers is used to investigate the steric effect in the cyclizations. Next, the non-spin-polarized and spin polarized Fukui functions for a radical attack on the radical conformer minima close to the transition state are computed, in analogy with an earlier study of De Proft et al. [32, 33]. Both the linear ground state conformations (Figure 4.2) and reactive conformations (Figure 4.3) –designated as the reactive rotamers, not the structures corresponding to the global minima– of the radicals are used for the calculation of the energies and reactivity indices. The reactive rotamers were investigated in detail recently [34], however the linear conformers were not. The 3D structures corresponding to the global minima of the linear conformations L1 through L11, and reactive rotamers of monomers R1 through R11 can be found in Figure 4.3 and 4.4. In order to gain a more detailed insight into the polar factors controlling the exo vs. endo mode of cyclization, the Fukui functions were investigated along the reaction path in the case of two prototypical cyclization reactions, for R4 and R10. Finally, the spin-polarized dual descriptor of the radicals is computed and plotted to investigate stereo-electronic effects on the regioselectivity.

23
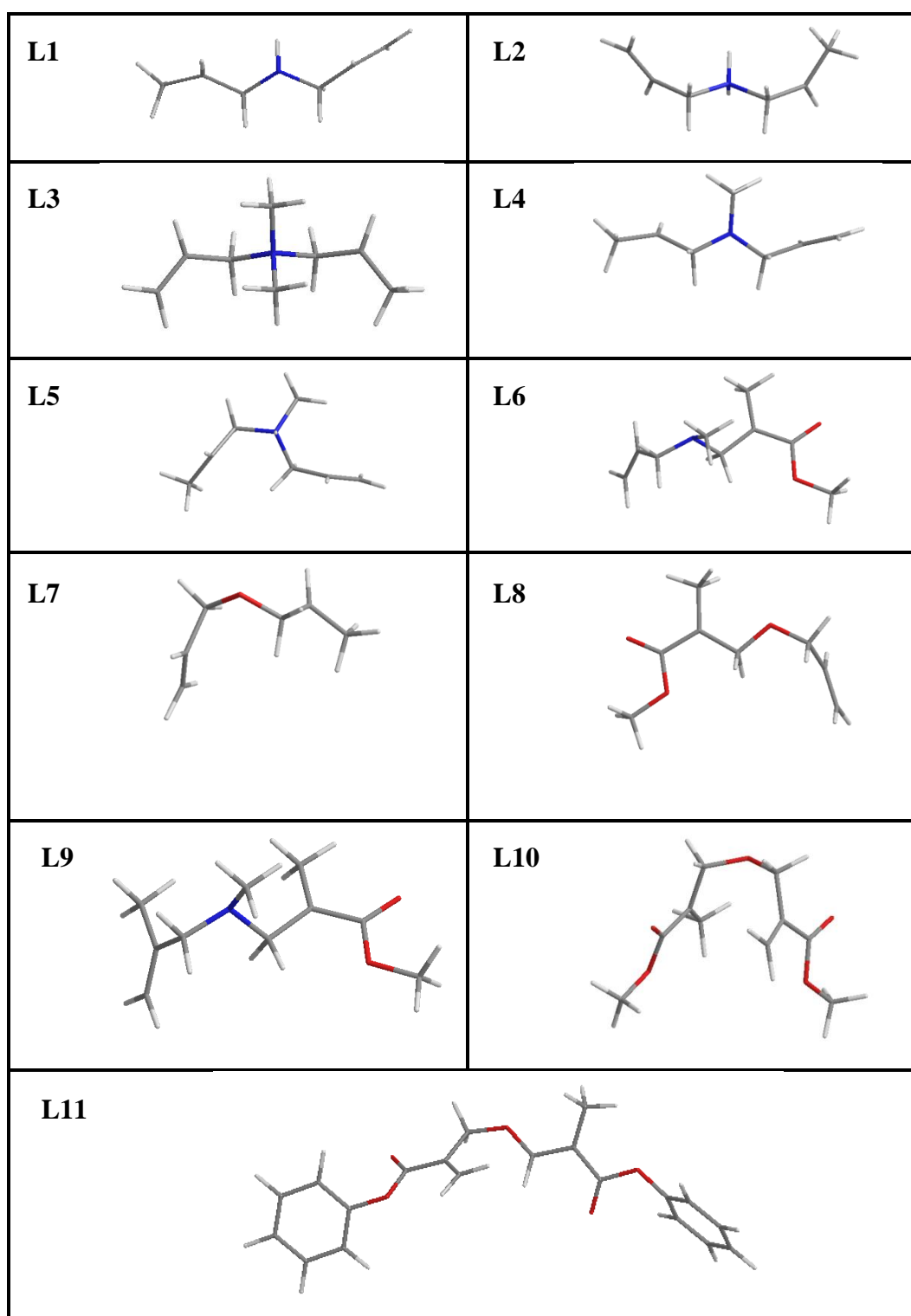
Figure 4.3. Linear conformer structures of the radicals of the selected diallyl monomers investigated in the present work.
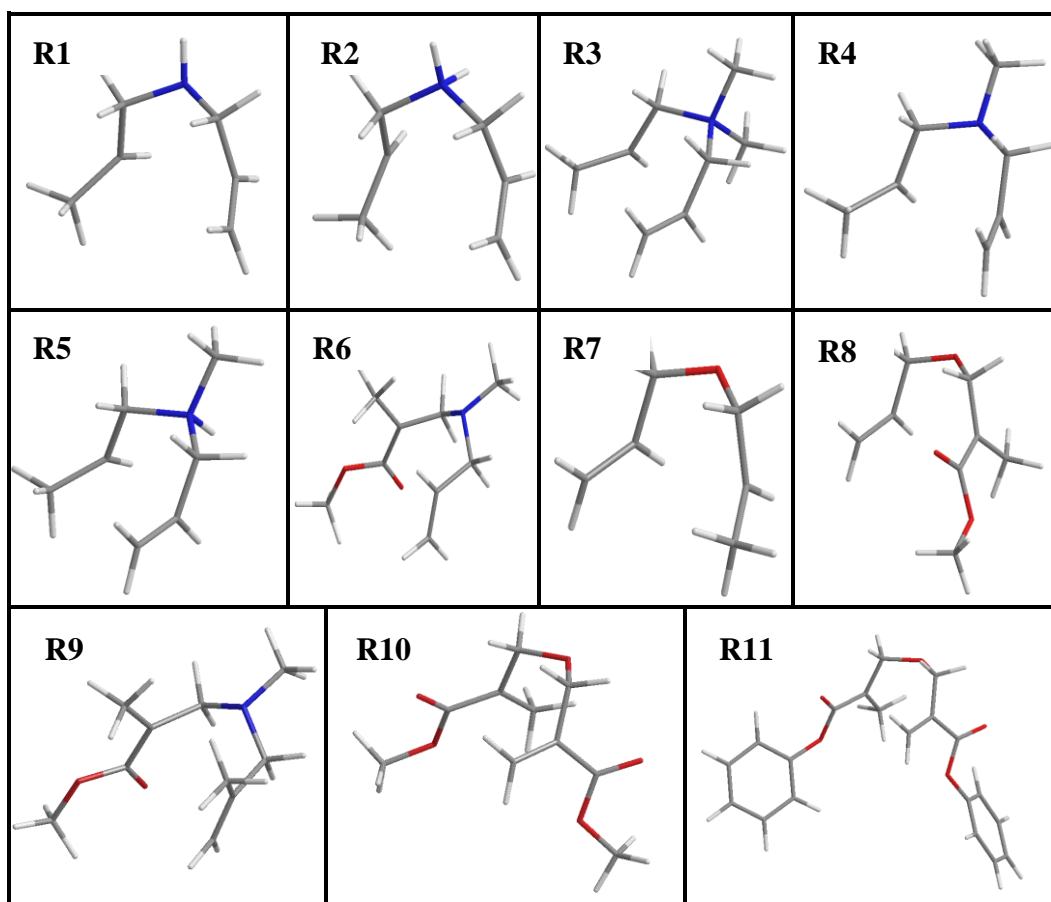
Figure 4.4. Reactive conformer structures of the radicals of the selected diallyl
monomers investigated in the present work.

4.2 Methodology

4.2.1 Computational Modeling

The most stable conformers of the model molecules were found by carrying out a
conformer search using the semi-empirical PM3 method by using the Spartan 06 program
package [35].

All calculations (ground state structures optimizations, transition state optimizations,
IRC calculations and electronic properties) were performed at the B3LYP [30] /6-
311++G(d,p) [36] level of theory using the Gaussian 03 program [37]. Atomic electron
populations and spin densities were obtained within the NPA scheme [38-40]. Single-point
energies in DMSO making use of the integral equation formalism-polarizable continuum

(IEF-PCM) model [39-42] at the B3LYP/6-311++G(d,p) level of theory have been calculated.

The energetic results are reported as the change in the electronic energy at 298 K (ΔE_{298}), sum of the electronic energy and zero point energy at 298 K ($\Delta E_{298+ZPE}$).

The activation energies were calculated as the difference between the energy of the transition state and the reactants.

4.2.2 Derivation of the descriptors

Different effects influencing the regioselectivity of the cyclization of the radicals derived from diallyl radicals will be investigated using concepts introduced in DFT based reactivity theory ("conceptual DFT") [45-52]. A central quantity often used in studies of regioselectivity is the Fukui function $f(r)$ introduced by Parr and Yang and defined as the initial response of the electron density due to an infinitesimal perturbation in the total number of electrons N, at constant external potential $\vartheta(r)$ [53, 54]

$$f(r) = \left[\frac{\delta \rho(r)}{\delta N}\right]_{v} \tag{4.1}$$

Due to the discontinuity of the electron density with respect to the number of electrons, [53, 54] three different Fukui functions can be introduced, representing the case of a nucleophilic attack $f^{+}(r)$, an electrophilic attack $f^{-}(r)$ or a neutral (radical) attack $f^{0}(r)$. For a system of N electrons, these can be computed as

$$f^{+}(r) = q_{N+1}(r) - q_{N}(r) \tag{4.2}$$

$$f^{-}(r) = q_{N}(r) - q_{N-1}(r) \tag{4.3}$$

and

$$f^{0}(r) = \frac{f^{+}(r) + f^{-}(r)}{2} \tag{4.4}$$

i.e. the average of the Fukui functions for an electrophilic and a nucleophilic attack. In these equations, $r_{N+1}(r)$, $r_N(r)$ and $r_{N-1}(r)$ represent the electron densities of the $N+1$, N and $N-1$ electron system computed at the geometry of the N electron system. High values of these quantities imply high probabilities of a nucleophilic, electrophilic or radical attack respectively. The derivative of the Fukui function with respect to the number of electrons is the so-called dual descriptor of chemical reactivity $f^{(2)}(r)$[57]

$$f^{(2)}(r) = \left[\frac{\delta f(r)}{\delta N}\right]_\vartheta \approx f^+(r) - f^-(r) \tag{4.5}$$

Among other things, the dual descriptor is useful for casting the famous Woodward-Hoffmann rules for pericyclic reactions in conceptual DFT [58]. $f^{(2)}(r)$ will be positive in regions of a molecule that are better at accepting electrons than they are at donating electrons, whereas $f^{(2)}(r)$ will be negative in regions that are better at donating electrons than they are at accepting electrons. It is then stated that favorable chemical reactions occur when regions that are good electron acceptors ($f^{(2)}(r) > 0$) are aligned with regions that are good electron donors ($f^{(2)}(r) < 0$) [57, 58].

In order to gain insight into the global electrophilic nature, we have also computed the global electrophilicity index of these radicals, a quantity that was introduced by Parr et al. as [59,60]

$$\omega = \frac{\mu^2}{2\eta} \tag{4.6}$$

where μ is the electronic chemical potential [61] and η is the chemical hardness [62-64]. This quantity was computed using a finite difference approximation for μ and η as [59]

$$\omega \approx \frac{(I+A)^2}{8(I-A)} \tag{4.7}$$

where I and A are the vertical ionization energy and electron affinity respectively.

All of these chemical concepts can be generalized in the framework of the so-called spin-polarized conceptual DFT [65, 66, 67]; in this representation, changes from one ground state to another are written in terms of the changes of N, v and N_s, the spin number which is the difference between the number of α and β spin electrons. (An equivalent representation uses N_α, N_β and v [66,67,68]). In this framework, the Fukui function f_{NN} can be written as [67, 68]

$$f_{NN}(r) = \left[\frac{\delta\rho(r)}{\delta N}\right]_{N_s,v} \tag{4.8}$$

which can be proven to be equal to [68]

$$f_{NN}(r) = \frac{1}{2}\left[f_{\alpha\alpha}(r) + f_{\alpha\beta}(r) + f_{\beta\alpha}(r) + f_{\beta\beta}(r)\right] \tag{4.9}$$

The Fukui functions in the $\{N_\alpha, N_\beta, v\}$ representation are defined as follows:

$$f_{\alpha\alpha}(r) = \left[\frac{\delta\rho_\alpha(r)}{\delta N_\alpha}\right]_{N_\beta,v}, f_{\alpha\beta}(r) = \left[\frac{\delta\rho_\alpha(r)}{\delta N_\beta}\right]_{N_\alpha,v}, f_{\beta\alpha}(r) = \left[\frac{\delta\rho_\beta(r)}{\delta N_\alpha}\right]_{N_\beta,v},$$

and

$$f_{\beta\beta}(r) = \left[\frac{\delta\rho_\beta(r)}{\delta N_\beta}\right]_{N_\alpha,v}$$

where ρ_α (ρ_β) is the density of the α (β)-electrons. The Fukui function for a radical attack is the average of the Fukui functions for a nucleophilic and an electrophilic attack

$$f_{NN}^0(r) = \frac{f_{NN}^+(r) + f_{NN}^-(r)}{2} \tag{4.10}$$

Also spin-polarized versions of the dual descriptor have been put forward recently [64, 67]. Since the present cyclization corresponds to the transfer of an α electron from the

α HOMO (mainly located on the radical center) to the α LUMO, the dual descriptor can be approximated by the difference of the densities of the α LUMO and HOMO densities

$$f_{\alpha\alpha\alpha}^{(2)}(r) = \left[\frac{\delta f_{\alpha\alpha}}{\delta N_\alpha}\right]_\vartheta \approx |\varphi_{LUMO}^\alpha(r)|^2 - |\varphi_{HOMO}^\alpha(r)|^2 \qquad (4.11)$$

4.3 Results and Discussion

4.3.1 Energetics and the Entropic Effect

Experimental polymerization studies carried out on compounds L1 to L11 (or R1 to R11) have shown that the radicals L1 to L8 (or R1 to R8) form exclusively five-membered rings in their polymer backbones whereas radicals L9 to L11 (or R9 to R11) form six-membered ring structures [33, 70, 71].

Table 4.1. Energetics (kcal/mol) for cyclization of the radicals − linear conformations

(B3LYP/6-311++G(d,p)) (T=298.15 K for $\Delta G^{\neq}$ and $\Delta H^{\neq}$)

| Radical | $\Delta E^{\neq}$ (gas) | | $\Delta H^{\neq}$ | | $\Delta G^{\neq}$ | |
	$\Delta E^{\neq}$ (exo)	$\Delta E^{\neq}$ (endo)	$\Delta H^{\neq}$ (exo)	$\Delta H^{\neq}$ (endo)	$\Delta G^{\neq}$ (exo)	$\Delta G^{\neq}$ (endo)
L1	8.9	12.9	7.9	11.8	11.0	15.0
L2	10.0	13.2	8.9	12.0	12.6	15.9
L3	6.8	11.1	5.9	10.1	8.8	13.2
L4	6.3	11.9	5.3	10.8	8.3	13.9
L5	7.5	11.4	6.6	10.4	9.6	13.6
L6	9.8	13.3	8.9	12.3	12.2	15.9
L7	6.6	11.7	5.6	10.6	8.7	14.2
L8	11.5	14.4	10.4	13.3	14.1	17.3
L9	15.3	12.5	14.3	11.6	18.1	15.1
L10	14.7	9.5	13.8	8.5	18.0	12.3
L11	17.2	10.7	16.3	9.6	20.9	14.4

Table 4.2. Energetics (kcal/mol) for cyclization of the radicals – reactive conformations

(B3LYP/6-311++G(d,p)) (T=298.15 K for $\Delta G^{\neq}$ and $\Delta H^{\neq}$)

Radical	$\Delta E^{\neq}$ (gas)		$\Delta E^{\neq}$ (DMSO)		$\Delta H^{\neq}$		$\Delta G^{\neq}$	
	$\Delta E^{\neq}$ (exo)	$\Delta E^{\neq}$ (endo)	$\Delta E^{\neq}$ (exo)	$\Delta E^{\neq}$ (endo)	$\Delta H^{\neq}$ (exo)	$\Delta H^{\neq}$ (endo)	$\Delta G^{\neq}$ (exo)	$\Delta G^{\neq}$ (endo)
R1	6.8	10.8	6.9	10.7	5.8	9.7	8.9	12.9
R2	6.6	9.8	5.1	9.2	5.6	8.7	8.6	11.9
R3	4.5	8.8	4.0	8.6	3.6	7.9	6.0	10.4
R4	4.7	10.3	4.8	10.1	3.8	9.3	6.4	12.1
R5	5.2	9.1	3.8	8.9	4.3	8.2	7.0	11.0
R6	8.9	12.5	9.0	12.6	8.0	11.5	10.9	14.6
R7	5.7	10.8	5.7	11.0	4.7	9.7	8.0	13.5
R8	10.0	12.9	9.8	12.9	9.1	11.9	12.1	15.3
R9	13.8	11.0	14.0	10.6	12.9	10.1	16.0	12.9
R10	13.9	8.7	16.2	8.7	13.0	7.8	17.4	11.7
R11	15.2	8.7	15.7	8.6	14.5	7.8	18.0	11.5

When the energetics of activation of the cyclopolymerization reaction are considered (Table 4.1 and 4.2), for the radicals that undergo exo-cyclization (L1 up to L8 or R1 up to R8), the exo mode of cyclization has a lower activation barrier than the endo mode. For the radicals that undergo endo-cyclization (L9 up to L11 or R9 up to R11), the trend reverses such that the endo mode has a lower activation barrier. The enthalpy and free energy of activation follow the same trend (Table 4.1 and 4.2). Note that zero-point energies are included in all the values. This trend survives when the solvent is included in the calculations via the use of a continuum model for the reactive rotamers (Table 4.2). In this study, because all model monomers and their polymers are water soluble, dimethylsulfoxide (DMSO) is chosen as a polar solvent with a dielectric constant $\epsilon = 48$. It is also one of the solvents which has been used for the cyclopolymerization reactions of diacrylamide [72], methacrylic anhydride [73], diallylamine hydrochloride with sulfur dioxide [74], DADMAC with sulfurdioxide [75], and some diallylamine derivatives [76]. As seen in Table 4.2, the energy barriers are consistent with the experimental observations. Activation energies of the linear conformers were not calculated since the focus point of this study is the activation energies of the reactive conformers as mentioned before.

The contribution of entropy to the regioselectivity has also been investigated because the unexpected exo preference of hexenyl systems has been attributed to favorable activation entropy in the literature [77]. The entropies of activation of the exo vs. endo cyclizations considered in this work are listed in Table 4.3 -for linear conformations and Table 4.4 -for reactive rotamers. Indeed, the entropy of activation for the cyclization of L1 through L8 (or R1 through R8) is lower in the exo mode than in the endo mode; this trend is reversed for L9 and L10, but not for L11. This is also valid for reactive rotamers. Except for the L11 (or R11), all the radicals entropically favor the experimental pathway. Although the trend is consistent with the experimental ring size preference, the $\Delta\Delta S^{\neq}$ values are less than 1.15 (cal/mol K) which is far too small to be the dominant factor for the regioselectivity.

Table 4.3. Activation entropies (cal/mole K) for cyclization reactions - linear

conformations (B3LYP/6-311++G(d,p)).

Radical	$\Delta S^{\neq}$		$\Delta\Delta S^{\neq}$
	$\Delta S^{\neq}$ (exo)	$\Delta S^{\neq}$ (endo)	$\Delta S^{\neq}$ (exo)-$\Delta S^{\neq}$ (endo)
L1	-11.49	-12.07	0.57
L2	-13.56	-14.26	0.70
L3	-10.59	-11.27	0.68
L4	-10.83	-11.40	0.57
L5	-10.95	-11.55	0.60
L6	-12.16	-13.12	0.96
L7	-11.40	-13.01	1.61
L8	-13.51	-14.76	1.25
L9	-13.92	-12.69	-1.23
L10	-15.50	-13.81	-1.68
L11	-16.87	-17.53	0.66

Table 4.3. Activation entropies (cal/mole K) for cyclization reactions - reactive

conformations (B3LYP/6-311++G(d,p)).

Radical	$\Delta S^{\neq}$		$\Delta\Delta S^{\neq}$
	$\Delta S^{\neq}$ (exo)	$\Delta S^{\neq}$ (endo)	$\Delta S^{\neq}$ (exo)-$\Delta S^{\neq}$ (endo)
R1	-10.11	-10.64	0.52
R2	-10.08	-10.73	0.64
R3	-7.88	-8.51	0.62
R4	-8.78	-9.3	0.52
R5	-8.79	-9.34	0.55
R6	-9.6	-10.48	0.88
R7	-11.29	-12.77	1.47
R8	-10.19	-11.34	1.15
R9	-10.43	-9.3	-1.13
R10	-14.83	-13.28	-1.54
R11	-11.81	-12.42	0.61

4.3.2 Polar and stereo-electronic effects : Reactivity Indices

We will now investigate the regioselectivity of the cyclizations of the diallylmonomers central in this work using reactivity indices emerging from Density Functional Theory. In the first part, the polar and stereo-electronic effects and their role in explaining the observed regioselectivity will be examined. The global electrophilicities of the radicals, the Fukui functions for radical attack (both non-spin and spin-polarized), and the spin densities on the relevant atoms in the cyclization process were calculated for all radicals. For each radical, the indices are tabulated for three atoms; for the carbon bearing the radical center, the exo carbon (the carbon atom on the double bond which will form the 5-membered ring upon cyclization) and the endo carbon (the carbon atom on the double bond which will form 6-membered ring upon cyclization). The global electrophilicity values for all radicals indicate that these can be classified as being nucleophilic to neutral [78] except for high values associated with the radical cations L2, L3, L5 (Table 6) and R2, R3, R5 (Table 3). These electrophilicity values thus point to an interaction between the HOMO of the nucleophilic radical and the LUMO of the interested carbon with the double bond [76].

For all cases considered in this work, the Fukui functions are highest on the radical center which is the most reactive carbon. The second highest Fukui function values are on the endo-carbon atoms for all radicals, while the lowest values are on the exo-carbon atoms. Although the numerical values of these two quantities differ, this is the case for both the non-spin polarized (f^0) and the spin polarized (f_{NN}^0) Fukui functions. This fact shows that the Fukui functions favor the thermodynamic product, i.e. the formation of the six-membered ring.

Table 4.4. Reactivity indices: Global electrophilicity (GE) -linear conformations

Radicals	GE
L1	0.8663
L2	4.8603
L3	4.5585
L4	0.8474
L5	4.5923
L6	1.4968
L7	0.8883
L8	1.26
L9	1.508
L10	1.6163
L11	1.718

Table 4.5. Reactivity indices: Global electrophilicity (GE) –reactive conformations

Radicals	GE
R1	0.801
R2	4.663
R3	4.331
R4	0.812
R5	4.155
R6	1.438
R7	0.896
R8	1.552
R9	1.408
R10	1.616
R11	1.84

Table 4.6. Reactivity indices: Fukui function f^0, spin polarized Fukui function f_{NN}^0, spin

density ρs (B3LYP/6-311++G(d,p)).-linear conformations

	f^0			f_{NN}^0			ρ_s		
Radicals	exo C	endo C	radical C	exo C	endo C	radical C	exo C	endo C	radical C
L1	-0.0119	0.0784	0.4888	-0.0135	0.0782	0.2452	-0.0018	0.0032	0.9282
L2	-0.0023	0.1039	0.4578	0.0966	0.1569	0.2439	-0.0064	0.0147	0.89
L3	-0.0081	0.0899	0.4842	0.1053	0.1633	0.2536	-0.0035	0.0086	0.8865
L4	-0.0135	0.0745	0.494	-0.0219	0.066	0.2477	-0.0017	0.0033	0.9267
L5	-0.0112	0.1026	0.4742	0.0989	0.1676	0.2457	-0.0059	0.0118	0.8947
L6	-0.0196	0.0643	0.3993	-0.0239	0.0576	0.1956	-0.0037	0.008	0.7358
L7	-0.0305	0.0372	0.5326	0.0024	0.0698	0.2714	0	0.0002	0.9242
L8	-0.0277	0.0461	0.38	0.0527	0.1231	0.1977	-0.001	0.0019	0.7214
L9	-0.005	0.0592	0.4005	-0.0061	0.0569	0.1961	-0.0027	0.0068	0.7365
L10	0.0023	0.0419	0.3986	0.0164	0.0934	0.2062	-0.0073	0.019	0.7358
L11	0.0003	0.0069	0.3341	0.0166	0.0623	0.1709	0	0.0003	0.7202

Table 4.7. Reactivity indices: Fukui function f^0, spin polarized Fukui function f_{NN}^0, spin

density ρs (B3LYP/6-311++G(d,p)).-reactive conformations

	f^0			f_{NN}^0			ρ_s		
Radicals	exo C	endo C	radical C	exo C	endo C	radical C	exo C	endo C	radical C
R1	-0.012	0.108	0.439	-0.007	0.094	0.222	-0.019	0.037	0.916
R2	-0.023	0.112	0.43	0.08	0.158	0.221	-0.021	0.044	0.888
R3	-0.019	0.123	0.461	0.086	0.158	0.235	-0.03	0.062	0.881
R4	-0.009	0.15	0.453	-0.015	0.103	0.228	-0.035	0.072	0.905
R5	-0.021	0.121	0.445	0.1	0.183	0.227	-0.026	0.053	0.892
R6	-0.014	0.083	0.398	-0.02	0.064	0.2	-0.019	0.042	0.73
R7	-0.01	0.132	0.464	0.021	0.12	0.237	-0.023	0.047	0.912
R8	-0.015	0.075	0.4	0.009	0.075	0.209	-0.013	0.029	0.735
R9	0.007	0.056	0.387	0	0.052	0.194	-0.009	0.03	0.732
R10	0.002	0.042	0.399	0.016	0.093	0.206	-0.007	0.019	0.736
R11	0.009	0.027	0.349	0.02	0.076	0.178	-0.007	0.019	0.727

Close inspection of the spin density shows that the radical center and the endo carbon have an excess of alpha spin and the exo carbon has an excess of beta spin. If spin-coupling between centers of opposite spin controlled the reactivity, then all radicals would undergo cyclization in the exo mode.
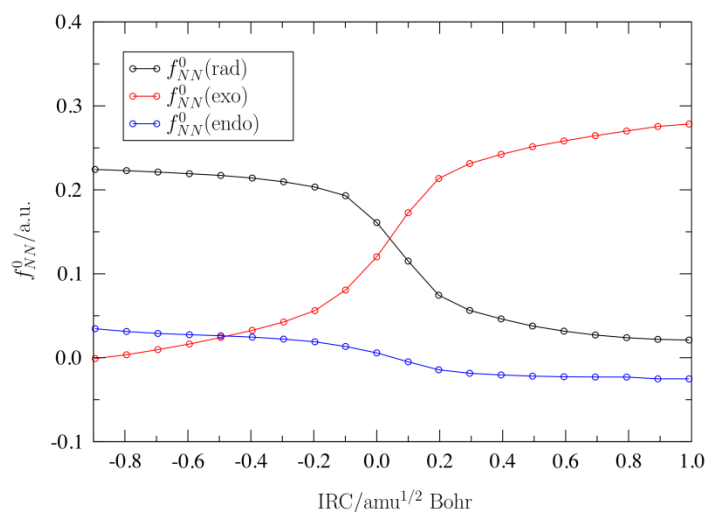
Figure 4.4 Evolution of the spin-polarized Fukui function for a radical attack f_{NN}^0 on the radical center, exo and endo carbon atoms along the endo (a) cyclization mode for radical R10
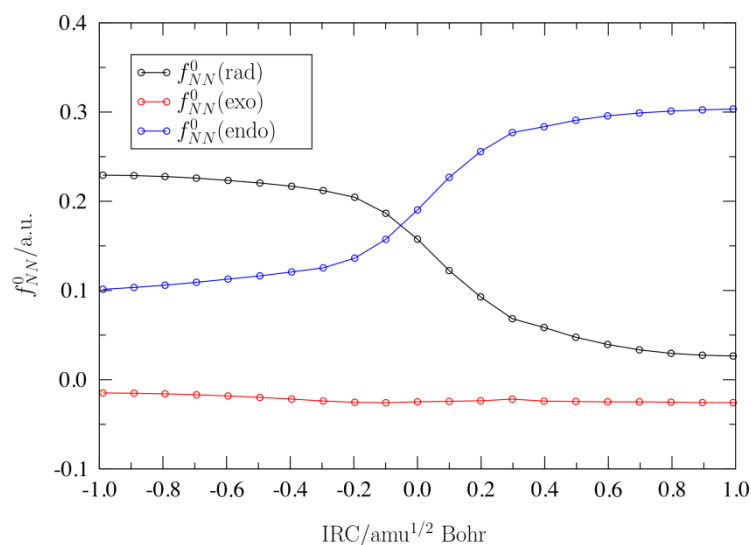

Figure 4.5. Evolution of the spin-polarized Fukui function for a radical attack f_{NN}^0 on the radical center, exo and endo carbon atoms along the exo cyclization mode of radical R4.

Insight in the observations made for the Fukui functions is obtained when considering the evolution of this quantity along the reaction path; we plot in Figure 4.4 and Figure 4.5 the evolution of f_{NN}^0 along the reaction profile for the endo cyclization mode for radical R10 (a compound with a preferred endo regioselectivity of cyclization) and the exo cyclization mode for radical R4 (a compound with a preferred exo regioselectivity of

cyclization). For the endo mode (IRC calculations starting from endo transition state) of the radicals (Figure 4.4) we observe that the Fukui function is initially always the highest on the radical center; the second highest value initially occurs on the endo carbon, whereas the exo carbon initially has the lowest value. During the reaction, the radical atom loses its reactivity and the exo carbon gains the reactivity. At the end of the reaction the exo carbon is the one with the highest reactivity which is meaningful since it is the new radical center for an endo cyclization path. When an exo cyclization is considered (Figure 4.5), at the beginning of the reaction, the radical center again has the highest value. The second highest value of the Fukui function is on the endo carbon and the exo carbon has the lowest value. Since it is an exo pathway, the second reactive carbon atom is supposed to be the exo carbon at the beginning of the reaction. So we can say that we don't have the correct information about the regioselectivity at the beginning of the reaction for the exo pathway. However, during the reaction, the reactivity of the endo carbon increases and at the end of the reaction the endo carbon becomes the highest reactive carbon atom which is again meaningful since the endo carbon is the new radical center for the exo pathway. Furthermore, for the endo pathway (Figure 4.4) the Fukui function on the exo carbon becomes larger than the endo carbon only very close to the transition state, this points to the fact that this transition state occurs much later than the exo transition state [70]. This is supported by the distance between the radical carbon and the exo carbon of the exo transition state geometry and the distance between the radical carbon and the endo carbon of the endo transition state geometry. In the "exo TS for R4" the distance between the radical carbon and the exo carbon is 2.244 Å; in the "endo TS for R4" the distance between the radical carbon and the endo carbon is 2.320 Å. In the "reactive rotamer for R4 (R10) the distance between the radical carbon and the exo carbon is 2.924 Å (3.251 Å), the distance between the radical carbon and the endo carbon is 3.604 Å (3.481 Å). Thus, in both cases during the cyclization, starting from the reactive rotamer, it is easier to reach the exo transition state than the endo transition state. We have observed the same trend for the other radicals as well.
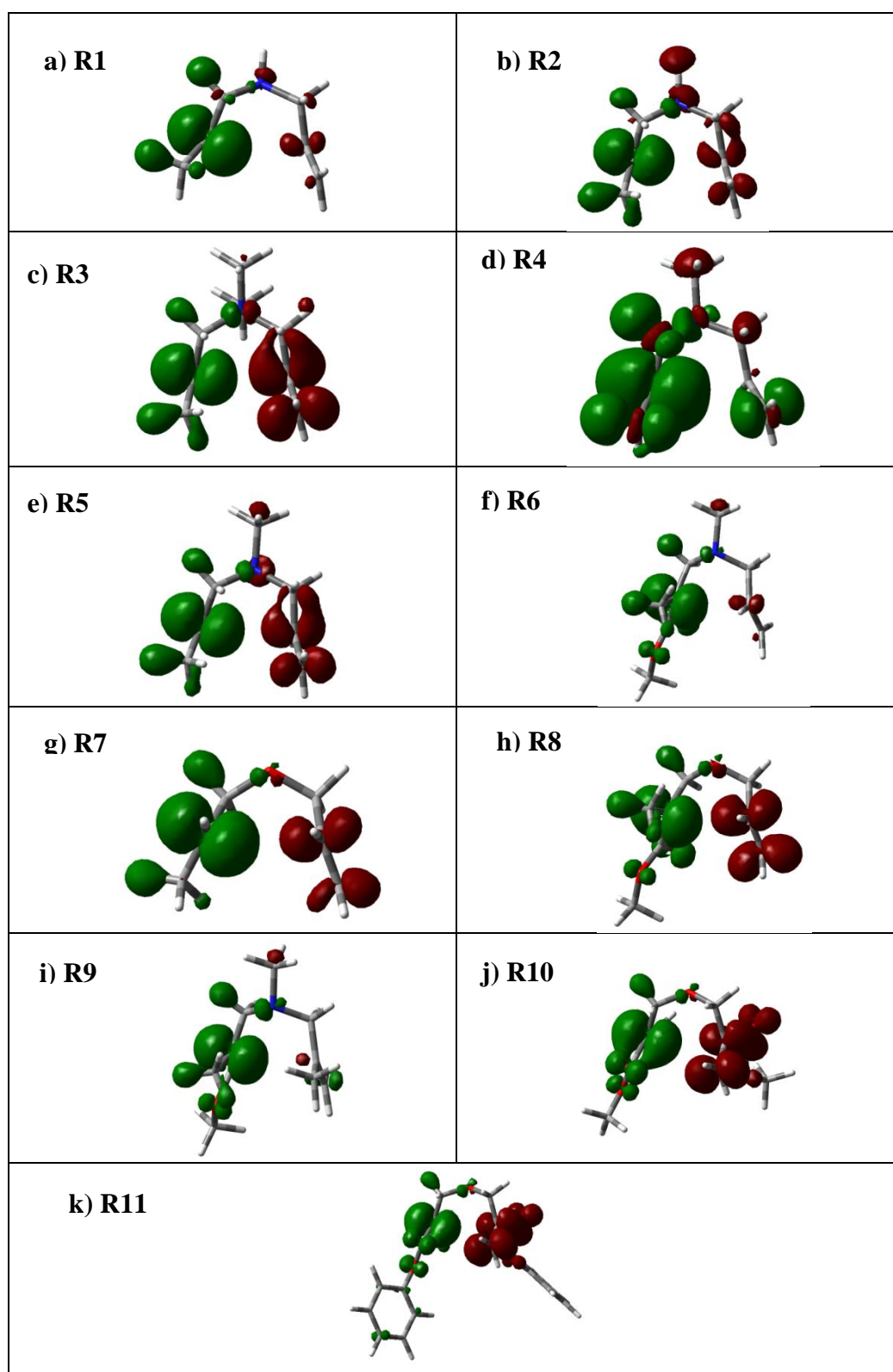
Figure 4.6. Spin-polarized dual descriptor $f_{\alpha\alpha\alpha}^{(2)}(r)$, as defined in Eq. (4.11), for all the radicals considered in this work. (isosurface value=0.0005)
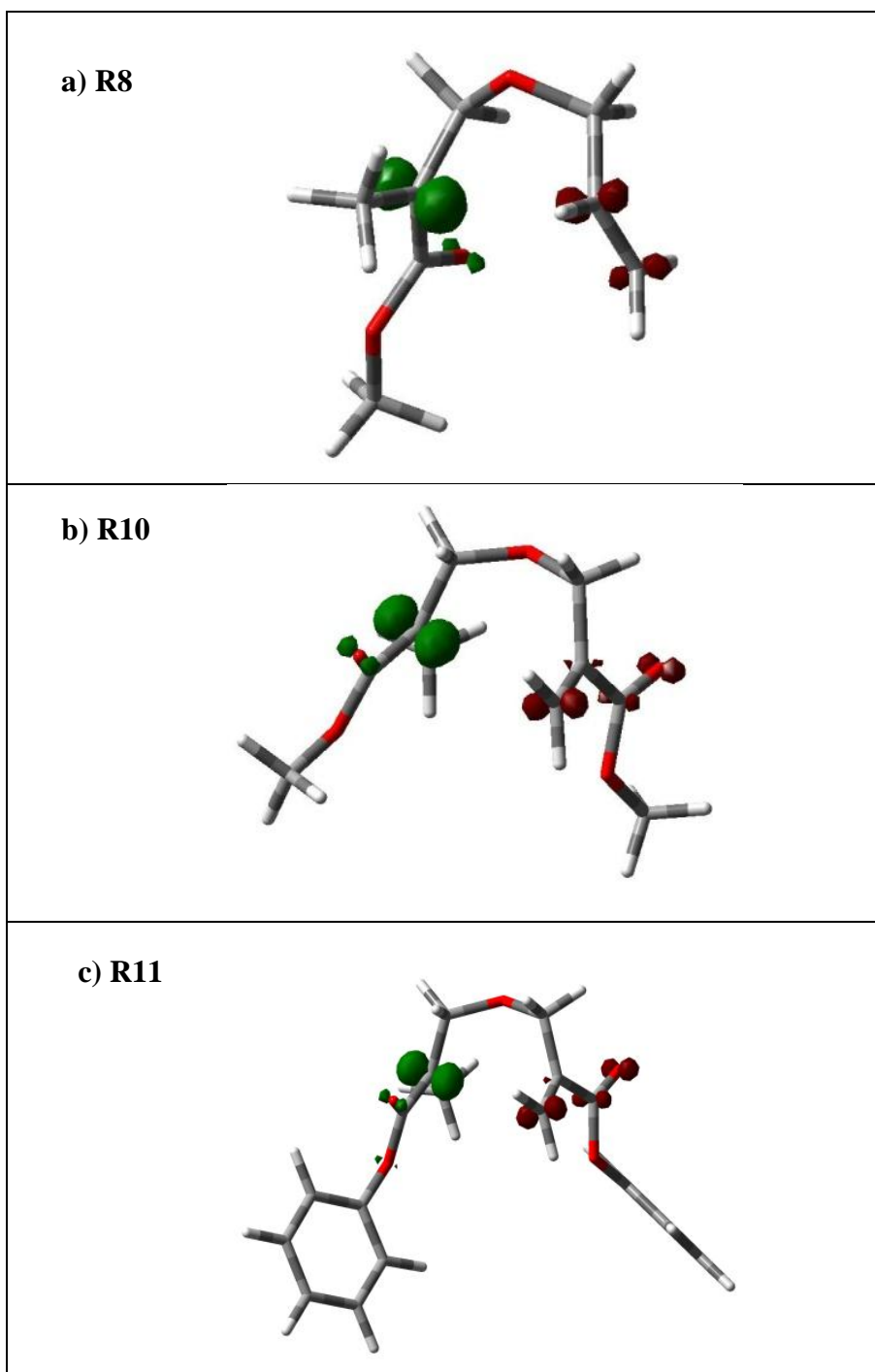
Figure 4.7. Spin-polarized dual descriptor $f_{\alpha\alpha\alpha}^{(2)}(r)$, as defined in Eq. (4.11), for all the radicals R8, R10, R11. (isosurface value=0.004)

Finally, we investigate whether the dual descriptor can specify the regioselectivity for the radical cyclization. In Figure 4.6 we have plotted the dual descriptors for all of the model radicals (isosurface value is 0.0005). For the radicals with a large number of heavy

atoms (R8, R10, R11) the isosurface value 0.0005 is not suitable enough to visualize the differences between endo and exo carbons. In Figure 4.7 dual descriptors for the radicals R8, R10 and R11 are reploted with the isosurface value 0.004 to visualize the dual descriptors properly. For four prototypical radicals considered in this work; the radicals R1 and R4 both show an exo regioselectivity in the cyclization, R10 and R11 prefer the endo pathway. For R1 in Figure 4.6, the region of the dual descriptor is larger around the exo carbon than around the endo one. Also there is a favorable alignment between the quantity on the radical center (green colored) and the exo carbon (red colored). For the R4 case in Figure 4.6.d, the lobe on the exo carbon cannot be visualized with these iso values; however, the repulsive interaction between the radical and the endo carbon can be seen. When the iso values are decreased, a small red colored region can be seen on the exo carbon. These results show that according to the dual descriptors, these two radicals undergo exo cyclization which is consistent with the experimental results. The same conclusions are reached for the other radicals, R2, R3, R5, R6, R7, R8, that are experimentally observed to undergo exo cyclization.

For R10 and R11, in Figures 4.6.j (or Figure 4.7.b) and 4.6.k (or Figure 4.7.c), the dual descriptor region around the endo carbon is larger than the one around the exo carbon. There is a favorable interaction between the orbital on the radical center (green colored) and the endo carbon (red colored). These results show that R10 and R11 undergo endo cyclization which is again consistent with the experimental findings. It can thus be concluded that the spin-polarized dual descriptor, introduced in Eq. (4.11), captures the stereo-electronic effects determining the regioselectivity in these radical cyclizations. The only exception is R9 in Figure 4.6.i which displays the endo reaction pathway and where the dual descriptor points to the exo carbon as the preferred carbon for cyclization.

4.4 Conclusions

Both linear, L1 to L11, and reactive conformations, R1 to R11, of eleven representative radicals were scrutinized to explore the regioselectivity in the cyclopolymerization reactions of diallyl monomers. The calculated activation barriers, activation enthalpies, and Gibb's Free energies support the experimental trend that shows that L1-L8 and R1-R8 form five-membered ring structures L9-L11 and R9- R11 form six-membered ring structures. The same observation holds for the entropies of activation - except for L11 and R11. The energy partitioning of the activation barriers shows that for the systems investigated, the regioselectivity cannot be explained by the steric effect, but that instead a nice linear relationship between the barrier differences and the electrostatic contributions can be established. The non-spin polarized (f^0) and spin polarized Fukui function ($f_{NN}{}^0$) values of the reactive rotamers, used as descriptors of the polar effect in these cyclizations, do not reproduce the experimental regioselectivity since both favor the formation of the six-membered ring in all cases. Conversely, the spin densities ρ_s favor the five-membered ring structure. Examining the spin polarized Fukui function ($f_{NN}{}^0$) along the reaction path has allowed to observe the reactivities of the carbon atoms for the model radicals R4 and R10. In both cases, the Fukui indices along the whole reaction pathway depict the regioselectivities. Finally, the dual descriptor ($f_{\alpha\alpha\alpha}^{(2)}(r)$) measuring stereo-electronic effects and computed in the framework of spin-polarized conceptual DFT, has been found to explain the regioselectivity. The positive overlap between the radical center and the exo carbon for the radicals R1 to R8 and the positive overlap between the radical center and the endo carbon for the radicals R10 to R11 confirm the experimental findings. Radical R9 is the only exception to the predicted reactivity based on dual descriptor analysis.

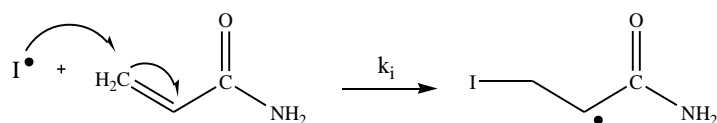# 5. FREE RADICAL POLYMERIZATION OF ACRYLAMIDE

5.1 Introduction

Free radical polymerization (FRP) is the most common method of chain growth polymerization. Interest in free radical polymerization derives from its effective usage in the field of polymerization. FRP can be used for any synthesizes by using unsaturated monomers such as: acrylates, acetates, styrene, ethylene…etc. The products of these polymerization reactions can be used in a variety of areas such as; medicine, construction, cleaning agents… etc. [79].

One of the most important concepts in free radical polymerization is the control of the reaction by chain transfer methods. The process of chain transfer is used to control mostly the molecular weight, the structure and in some cases the functionality. The classical method of controlling the molecular weight of polymer products is by adding the chain transfer agents to the reaction medium.
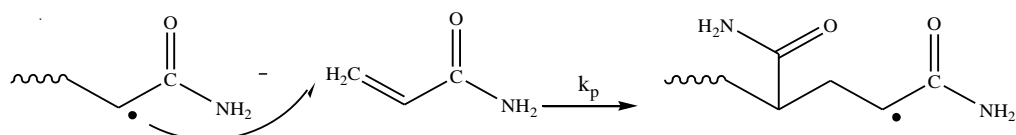
In this study, the free radical polymerization of acrylamide was investigated. Polyacrylamide, and copolymers of polyacrylamide have received considerable attention because they reached large-scale industrial use such as wastewater treatment, soil erosion control, cosmetic additive, drug design etc. [80-84].

The mechanism of the free radical polymerization of acrylamide is depicted in Figure 5.1.
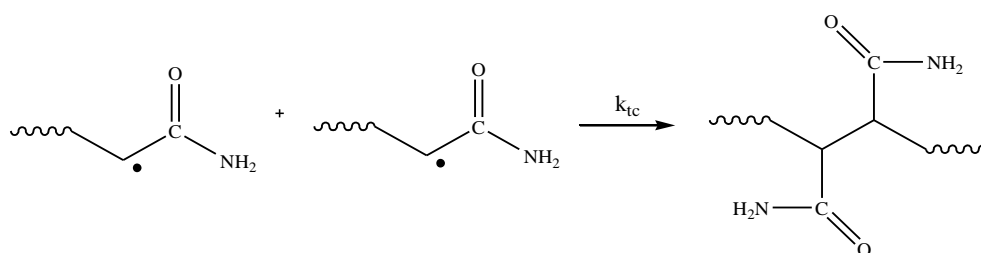
Initiation

Propagation

Termination by coupling
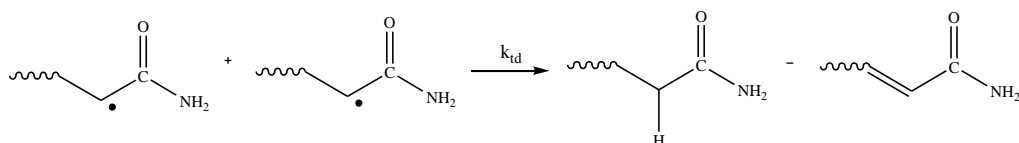

Termination by disproportionation

Figure 5.1. Free radical polymerization of acrylamide

When there are chain transfer agents in the polymerization medium, the termination reactions compete with the chain transfer reaction.
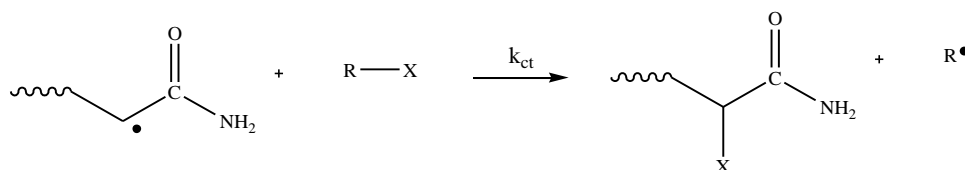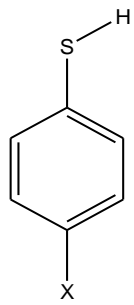
Figure 5.2. Chain transfer reaction of acrylamide

A number of thiophenols were used as chain transfer agents shown in Figure 5.3 [85]. Thiols are known as effective agents in chain transfer reactions for common monomers such as methyl methacrylate and styrene [86]. The weakness of the S-H bond [87] makes them efficient in the control of the chain length. The weakness of the S-H bond explains the high reactivity of these compounds towards chain radicals so the chain transfer reactions have high rate constants. Most of the reports on the behaviour of thiols as

chain transfer agents deal with aliphatic thiols [85]. In this study the efficiency of thiophenols as chain transfer agents was considered. The low energy of the S–H bond make these compounds more advantageous over the aliphatic thiols as chain transfer agents [85].

Names of Thiophenols	Substituent (X)
T1	-H
T2	$-NHCOCH_3$
T3	$-CH_3$
T4	$-OCH_3$
T5	-OH
T6	$-NH_2$

Figure 5.3. Chain transfer agents used in this study

The mechanism of the chain transfer reaction of the thiophenols has the same principle of the generic chain transfer reaction mechanism which was shown in Figure 5.2. In this case R-X is the thiophenols, and X is the H so that this reaction can be considered as an H abstraction reaction. (Figure 5.4)
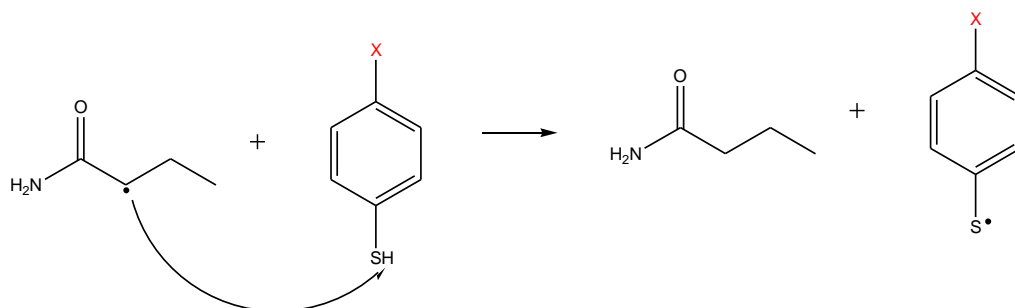

Figure 5.4. Chain transfer reaction between thiophenols and acrylamide radical.
(X=H, NHCOCH3, CH3, OCH3, OH, NH2)

In this study, the kinetics of the polymerization behavior and the chain transfer reactions of acrylamide was considered. Calculated propagation rate constants and the trend of rate of the chain transfer reactions have been compared with the experimental results.

5.2 Methodology

5.2.1 Computational Modeling

The most stable conformers of the model molecules were found by carrying out a conformer search using the semi-empirical PM3 method by using the Spartan 06 package [35].

All calculations (ground state structures optimizations and transition state optimizations) were performed at the B3LYP [30] /6-31+G(d) [36] level of theory using the Gaussian 03 program [37]. B3LYP can be considered as a good method for geometry optimizations [88]. For better energy calculations and more realistic kinetic data, different hybrid methodologies were tested such as: MPWB1K/6-311++G(3df,2p), M05-2X/6-311++G(3df,2p), and again B3LYP/6-311++G(3df,2p). MPWB1K is an example of DFT functionals for kinetics determined by a semiempirical approach [89]. Recent studies have shown that MPWB1K gives the best results for a combination of thermochemistry, thermochemical kinetics, hydrogen bonding, and weak interactions, especially for thermochemical kinetics and nonecovalent interactions [90]. M05-2X is a recently developed functional proposed by Truhlar et.al. in 2005 [89] M05-2X is a hybrid meta exchange-correlation functional which was designed for very general purposes such as; kinetics, thermochemistry of main group elements, noncovalent interactions, ionization potentials and activation energies [89]. The accuracy of this new method on H abstraction reactions was also investigated. For the activation energy barriers, it was found that this method is less accurate than BB1K, PWB6K, MPWB1K, MPW1K, BMK, for H-abstraction reactions, whereas much more accurate than the B3LYP and other functionals [89].

All the energetic results are reported as the change in the electronic energy at 298 K (ΔE_{298}), sum of the electronic energy and zero point energy at 298 K ($\Delta E_{298+ZPE}$).

5.2.2 Reaction Rate Calculations

The reaction rate constants are calculated by using the activated complex theory which enables the rate constants in chemical reactions to be calculated using statistical thermodynamics [91]. To correlate thermodynamics with rate constants the relation between equilibrium constant and partition functions should be investigated for a sample reaction:

$$aA + bB \; \rightarrow cC + dD$$
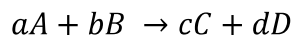
The equilibrium constant for this reaction is given by the expression:

$$K = \frac{(q_{C,m}^0/N_A)^c (q_{D,m}^0/N_A)^d}{(q_{A,m}^0/N_A)^a (q_{B,m}^0/N_A)^b} \; e^{-\Delta_r E_0/RT} \tag{5.1}$$

where $\Delta_r E_0$ is the difference in molar energies of the ground states of the products and reactants.

$$K^{\neq} = \frac{N_A q_{c^{\neq}}^0}{q_A^0 \; q_B^0} \; e^{-\Delta E_0/RT} \tag{5.2}$$

where

$$\Delta E_0 \; = \; E_0(C^{\neq}) - \; E_0(A) - E_0(B) \tag{5.3}$$

Partition function ($\bar{q}_{c^{\neq}}$) for all the modes of the complex can be denoted as:

$$q_{c^{\neq}} \approx \frac{kT}{h\upsilon} \; \bar{q}_{c^{\neq}} \tag{5.4}$$

The constant $K^{\neq}$ is therefore

$$K^{\neq} = \frac{kT}{h\upsilon}\,\overline{K}^{\neq} \tag{5.5}$$

$$\overline{K}^{\neq} = \frac{N_A \bar{q}^0_{c^{\neq}}}{q^0_A\,q^0_B}\,e^{-\Delta E_0/RT} \tag{5.6}$$

$$k = k^{\neq}\frac{RT}{P^0}\,K^{\neq} = K\,\upsilon\,\frac{kT}{h\upsilon}\frac{RT}{P^0}\overline{K}^{\neq} \tag{5.7}$$

By writing

$$\overline{K}^{\neq}_C = \left(\frac{RP}{p^0}\right)\overline{K}^{\neq} \tag{5.8}$$

We obtain the Eyring equation:

$$k = \kappa\,\frac{kT}{h}\,\overline{K}^{\neq}_C \tag{5.9}$$

With $\overline{K}^{\neq}_C$ a kind of equilibrium constant, but with one vibrational mode of $C^{\neq}$ discarded. Than the rate of equation can be written as:

$$k(T) = \frac{kT}{h}\frac{N_A \bar{q}^0_{c^{\neq}}}{q^0_A q^0_B}\,e^{-\Delta E_0/RT} \tag{5.10}$$

where k_B represents Boltzman's constant, T is the temperature, h is the Planck's constant, ΔE_0 represents the molecular energy difference between the activated complex and the reactants (with inclusion of zero point vibrational energies), and q_{TS}, q_A and q_B are the molecular partition functions of the transition state and reactants, respectively. Effects of tunneling on the rate constants are neglected. The activation energies, ΔE_0, are calculated

at 298 K. The partition functions are obtained from the Gaussian output and are evaluated at 298 K.

Chain transfer constants, C_{tr} can be computed as follows:

$$C_{tr} = \frac{k_{tr}}{k_p}$$
(5.11)

where k_{tr} is the chain transfer rate constant and k_p is the propagation rate constant.

5.3 Results and Discussion

5.3.1 Structural Analysis

The structure of the propagating acrylamide radical was considered by replacing the long polymer chain with a CH_3 fragment according to the reaction in Figure 5.5. Eventhough this chain does not mimic the actual polymer chain, this approach is cost effective. Also it was found in previous studies that this method is adequate for modeling the free radical polymerization reactions [92, 93].
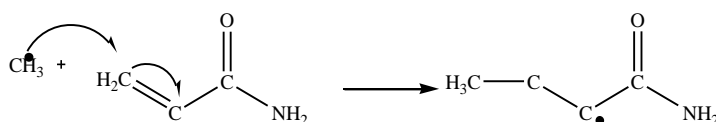

Figure 5.5. Initiation of the acrylamide monomer by CH3 radical.

Among the 3-dimensional structures for the polymerizing acrylamide radical (optimized with B3LYP/6-31+G(d)) AA-R-syn is the syn conformer of the acrylamide radical and AA-R-anti is the anti conformer The syn conformer was found to be lower in energy than the anti conformer by 1.28 kcal/mole. (Figure 5.6)

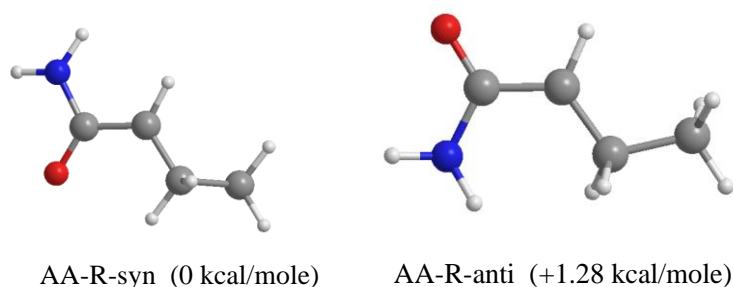AA-R-syn (0 kcal/mole)   AA-R-anti (+1.28 kcal/mole)

Figure 5.6. Relative energies and 3-D structures of acrylamide radical

In Figure 5.7 the transition state geometries of the propagation reaction are depicted in 3-D. Since the most stable geometry of the acrylamide radical was found as the syn conformer the transition state geometries with syn conformers of acrylamide radical were considered. For the structure TS-AA-syn-1, the dihedral between the atoms C1, C2, C3, and C4 is 100.22^0 and the dihedral for the same atoms is 177.82^0 for TS-AA-syn-2 , furthermore TS-AA-syn-2 is 0.40 kcal/mole higher in energy than TS-AA-syn-1. (Figure 5.7) This energy difference can be explained by the repulsive interaction of the terminal CH_3 with the monomer. Thus TS-AA-syn-1can be considered as the global minima of the transition state of the acrylamide propagation reaction. This result is consisted with the results of previous analysis on different radicals such as acrylates which was proposed by Aviyente et. al. [92, 93].

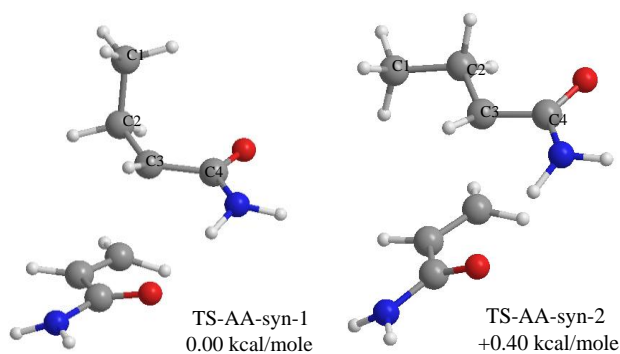TS-AA-syn-1
0.00 kcal/mole

TS-AA-syn-2
+0.40 kcal/mole

Figure 5.7. Relative energies and 3-D structures for the propagation reaction.

Relative energies of the transition state was investigated for the different values of the torsional angles between the monomer and the radical. The rotational potential for the propagation reaction was calculated by altering the C2 C3 C5 C6 dihedral by 200 in each

step and by calculating the energies of these local minima. The relative energy vs torsional energy plot (Figure 5.8) shows that the structure with the dihedral 71.970 is the global minimum for this transition state. This structure has an intermolecular hydrogen bond between the hydrogen (H1), bonded to the nitrogen atom of radical moiety, and the oxygen (O1) of the monomer with a close contact: 2.03 A. (Figure 5.8).
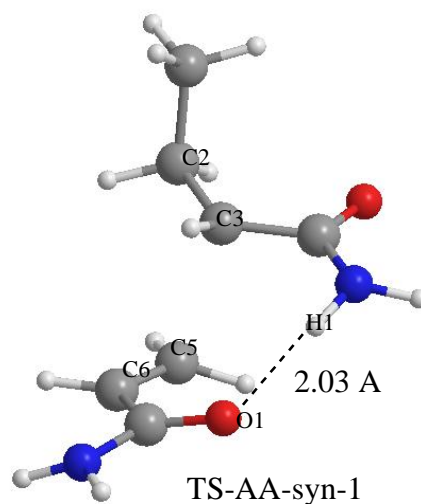
Figure 5.8. The most stable transition state geometry for the propagation reaction of acrylamide
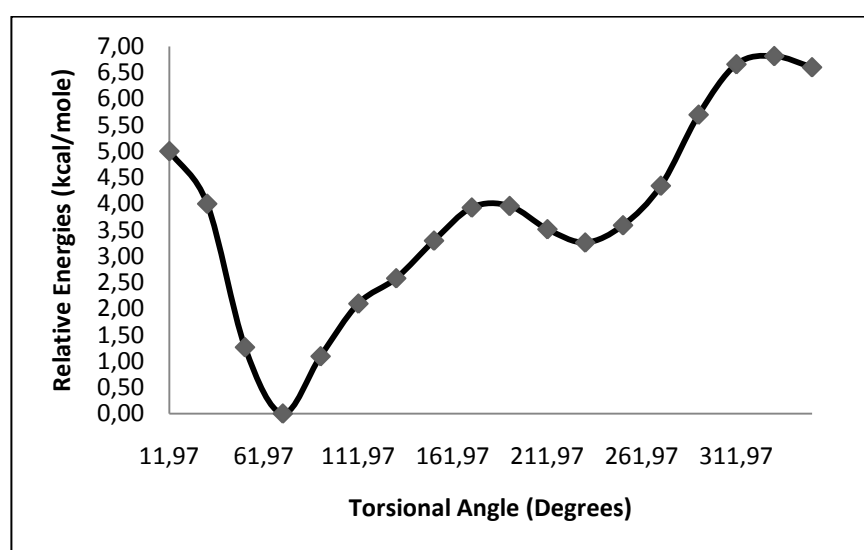
Figure 5.9. Relative Energy (/kcal/mole) vs torsional Angle (0) for the propagation reaction

For the chain transfer reactions, the structures of the acrylamide radical, thiophenols and the transition states of the chain transfer reaction should be examined, the radical AA-R-syn was used for all the calculations.

T1	T2
T3	T4
T5	T6

Figure 5.10. Most stable conformers of the thiophenols (Gray color represents carbon atom, white hydrogen, red oxygen, blue nitrogen and yellow sulphur)

Figure 5.11. Most stable conformers of the transition state structures (Gray color represents carbon atom, white hydrogen, red oxygen, blue nitrogen and yellow sulphur)

For the structures of the thiophenols it was found that there are two possibilities for the dihedral between H1, S, C1, and C2 (Figure 5.10). T1, T2, and T3 can be considered as planar structures, whereas for T4, T5, and T6 the S-H bond is perpendicular to the plane of the molecule. This finding can be attributed by the fact that T1, T2, T3 minimize their dipole in a planar structure, T4, T5, and T6 minimize their dipole with an S-H group perpendicular to the molecular plane.

AA-R-syn was used to generate the transition state geometries of the chain transfer reaction. The relative energies of the transition states were investigated for the different torsion angles between the monomer and the radical. TS1 was used as a model for analyzing the effect of torsional angle between the monomer and the radical. The dihedral between C1, S, C2, and C4 is 170.88° for TS1 (Figure 5.12). The relative energy vs torsional energy plot (Figure 5.13) shows that the structure with the dihedral 170.88^{0} corresponds to the global minimum for this transition state. This structure is stabilized by the interaction between the positively charged hydrogen (H1) atom, bonded to nitrogen of the radical, and the negatively charged carbon (C1) atom in the thiophenol ring. Mulliken charges on H1 and C1 are 0.41, and -0.114 respectively.
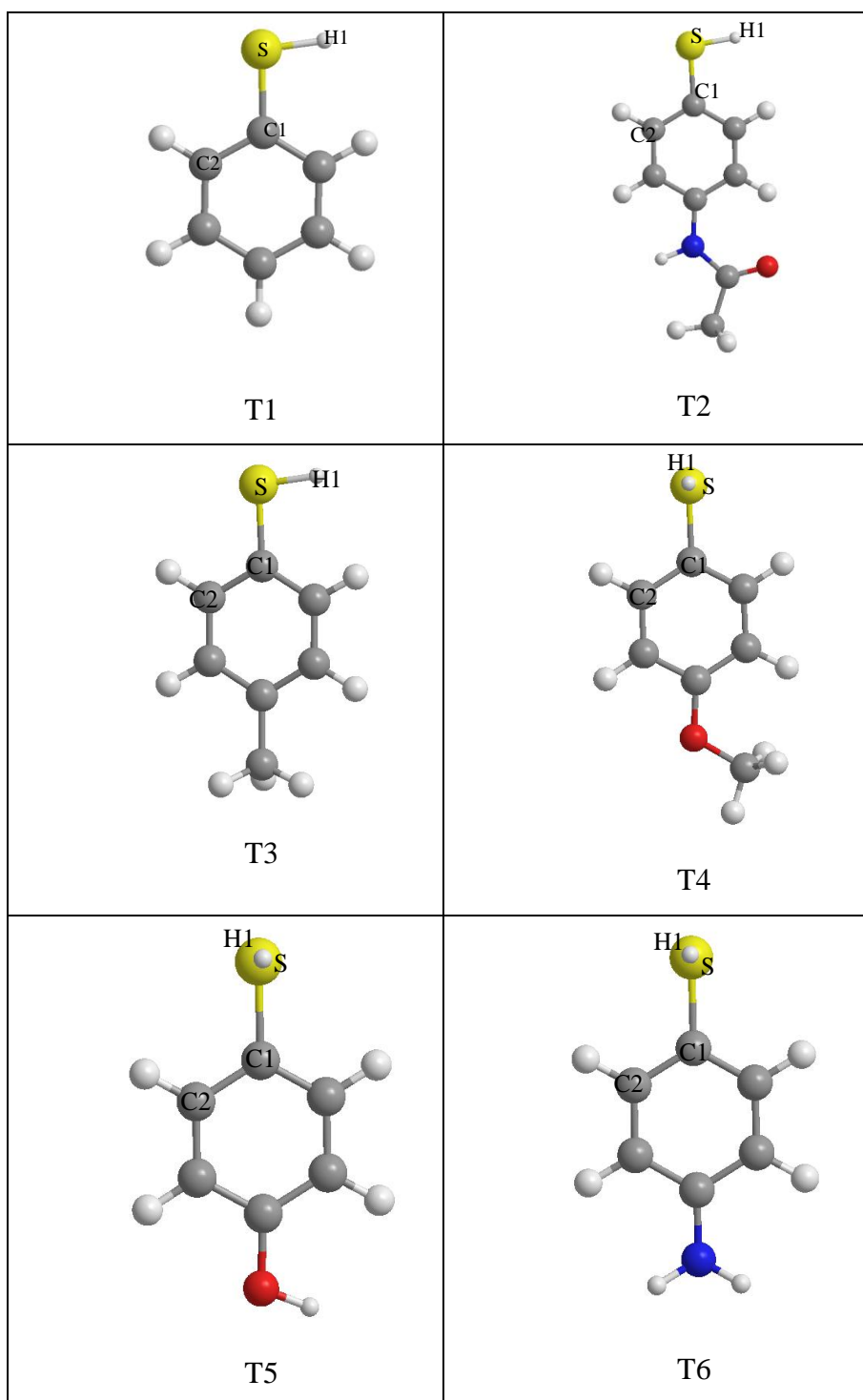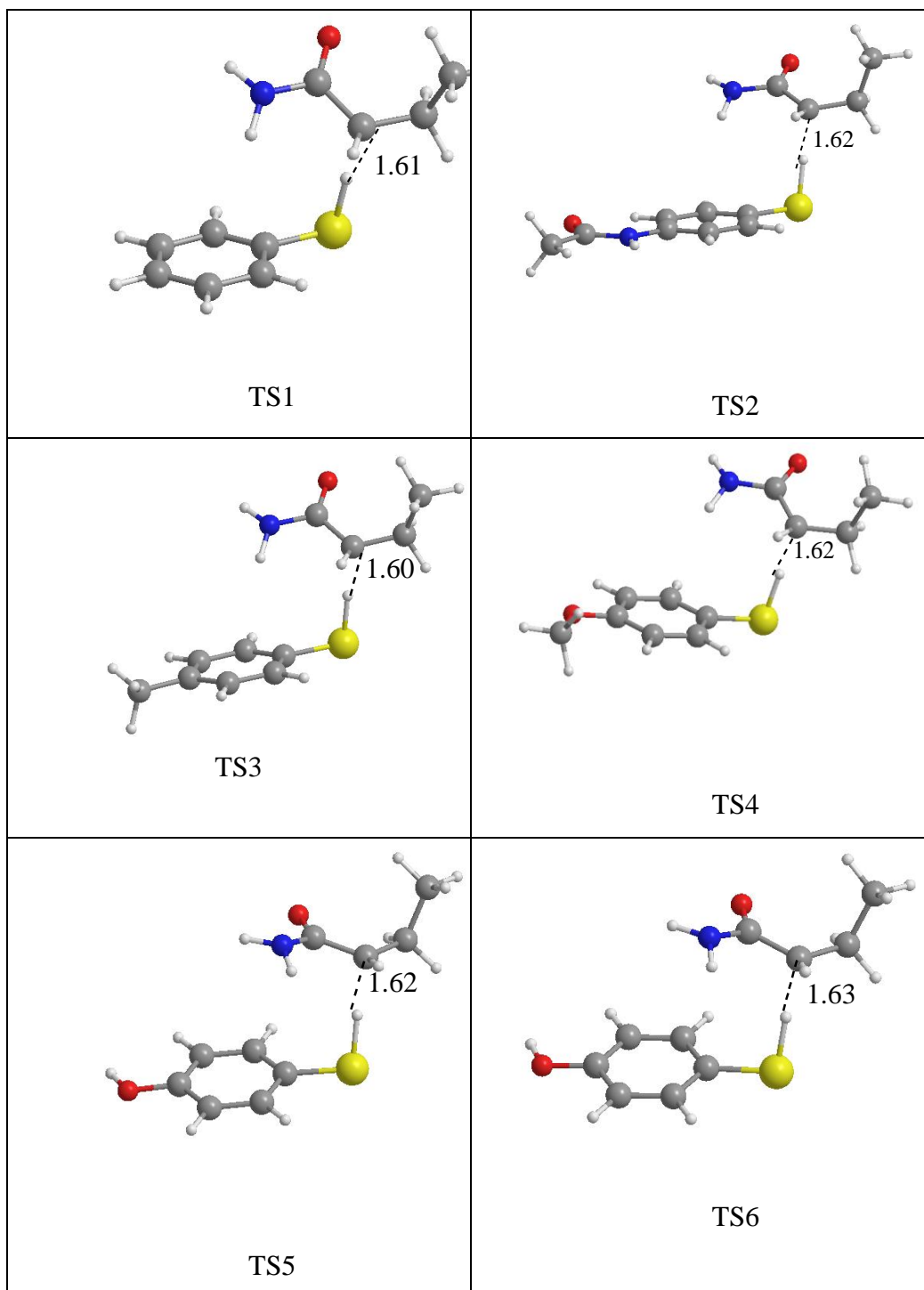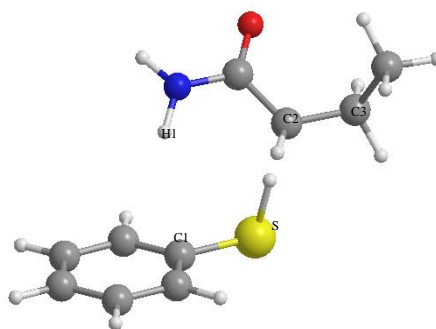

Figure 5.12. The most stable transition state geometry of chain transfer reaction for TS1
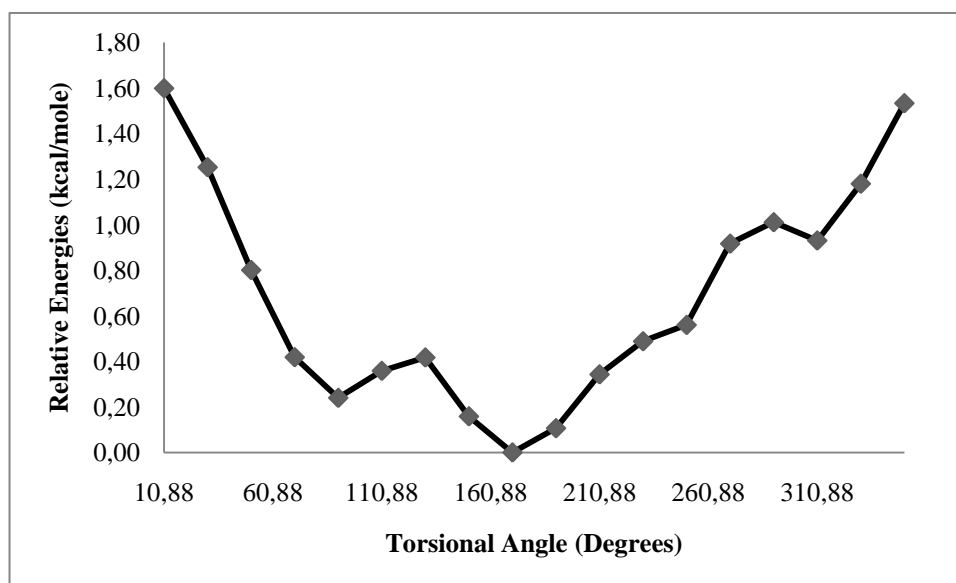
Figure 5.13. Relative Energy (kcal/mole) vs Torsional Angle (0) for the chain transfer reaction

5.3.2 Rate analysis

The propagation rate constant (k_p) of acrylamide polymerization reaction is calculated by using the equation 5.9. Rate constants were calculated by performing single point energy calculations with B3LYP/6-311++G(3df,2p), MPWB1K/6-311++G(3df,2p), and M05-2X/6-311++G(3df,2p) on the structures located with B3LYP/6-31+G(d). (Figure 5.15). The experimental rate of propagation of acrylamide in aqueous solution with pH 4.6 at 25^0C is $4.02E+03$ M^{-1} s^{-1}. [85]. The most accurate rate results in terms of magnitude were obtained with M05-2X/6-311++G(3df,2p) method with a value of $1.03E+02$ M^{-1} s^{-1}. (Table 5.1).

Table 5.1. Rate of propagation, k_p of acrylamide polymerization with different methods.

Methods	k_p (/M^{-1} s^{-1})
B3LYP/6-31+G(d)	3.00E-02
B3LYP/6-311++G(3df,2p)	4.74E-03
MPWB1K/6-311++G(3df,2p)	4.09E-01
M05-2X/6-311++G(3df,2p)	1.03E+02

Rate of chain transfer reaction (k_{ct}) is calculated by using the same equations for 6 different chain transfer agents with different substituents of thiophenols. The same calculations were performed by using the energies derived from B3LYP/6-311++G(3df,2p), MPWB1K/6-311++G(3df,2p), and M05-2X/6-311++G(3df,2p). The highest rate constant was obtained by using the molecule T6, which bears the strong electron donating NH_2 group, as a chain transfer agent.

Charge transfer effects associated with the reaction between a growing macroradical and the chain transfer agent can be quantified by the classical Hammett equation [94]

$$\log (k_{ct}) = \rho\sigma_P \tag{5.10}$$

In this expression, the Hammett constant σ_P is characteristic of the substituent at position 4, while the reaction constant ρ is characteristic of the reaction [94]. To investigate the effect of substituents of thiophenols the Hammet constants vs log (k_{ct}) values were also plotted. (Figure 5.15)

Table5.2. Calculated and experimental kct results

Substituents of thiophenols	k_{ct} exp [1]	k_{ct} Calculated			
		B3LYP*	B3LYP **	MPWB1K	M05-2X
-H	1150	6.41E+00	4.78E-01	1.57E+00	2.23E+02
-NHCOCH$_3$	800	9.76E+00	1.22E+00	3.37E+00	4.51E+02
-CH$_3$	1090	6.01E+00	4.62E-01	1.53E+00	2.11E+02
-OCH$_3$	1650	1.73E+01	2.51E+00	4.09E+00	4.04E+02
-OH	2600	1.53E+01	2.34E+00	6.53E+00	3.27E+02
-NH$_2$	10900	4.50E+01	5.94E+00	1.52E+01	1.10E+03
* B3LYP/6-31+G(d), ** B3LYP/6-311++G(3df,2p)					
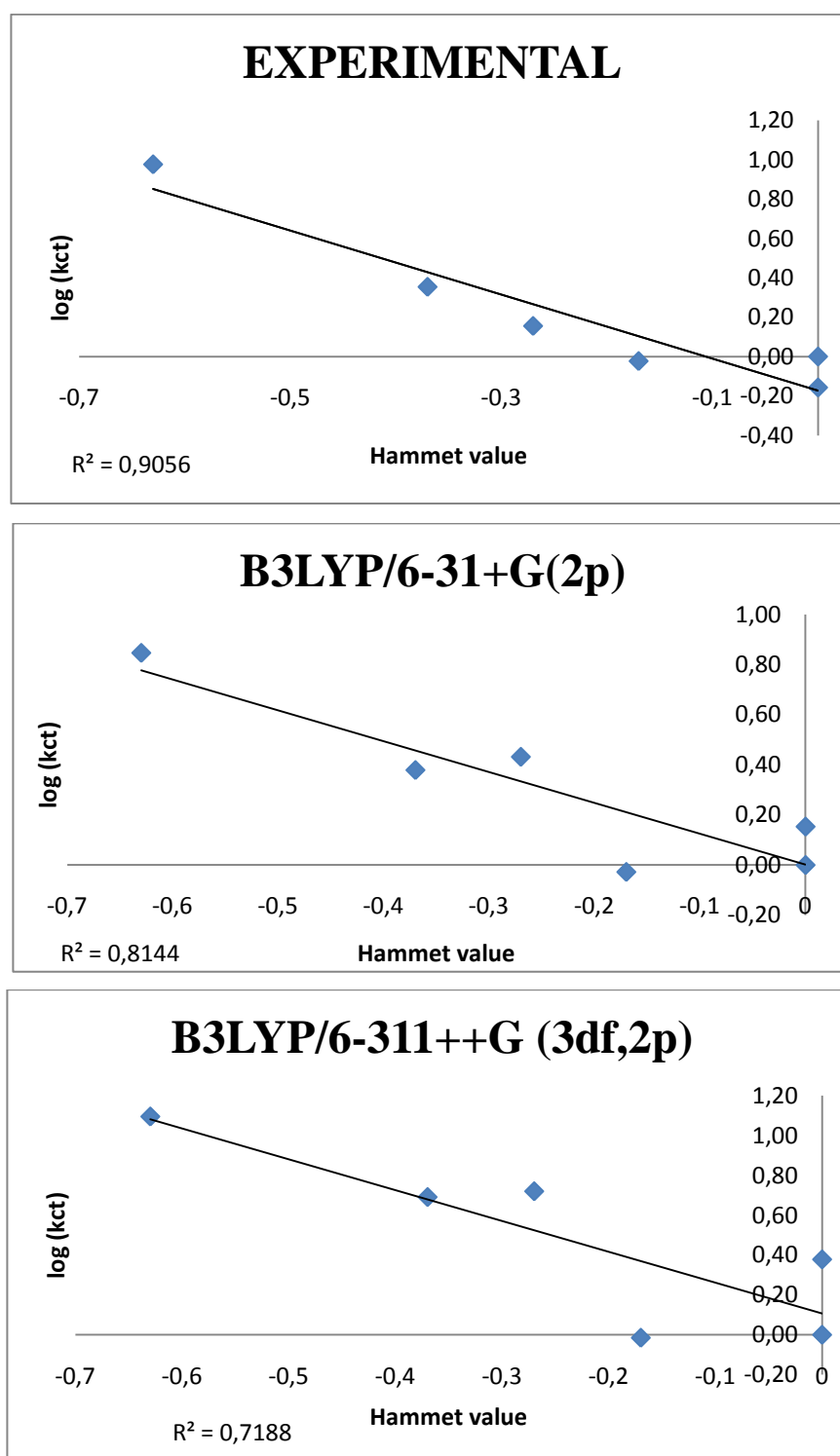
Figure 5.14. Hammet values vs k_{ct}
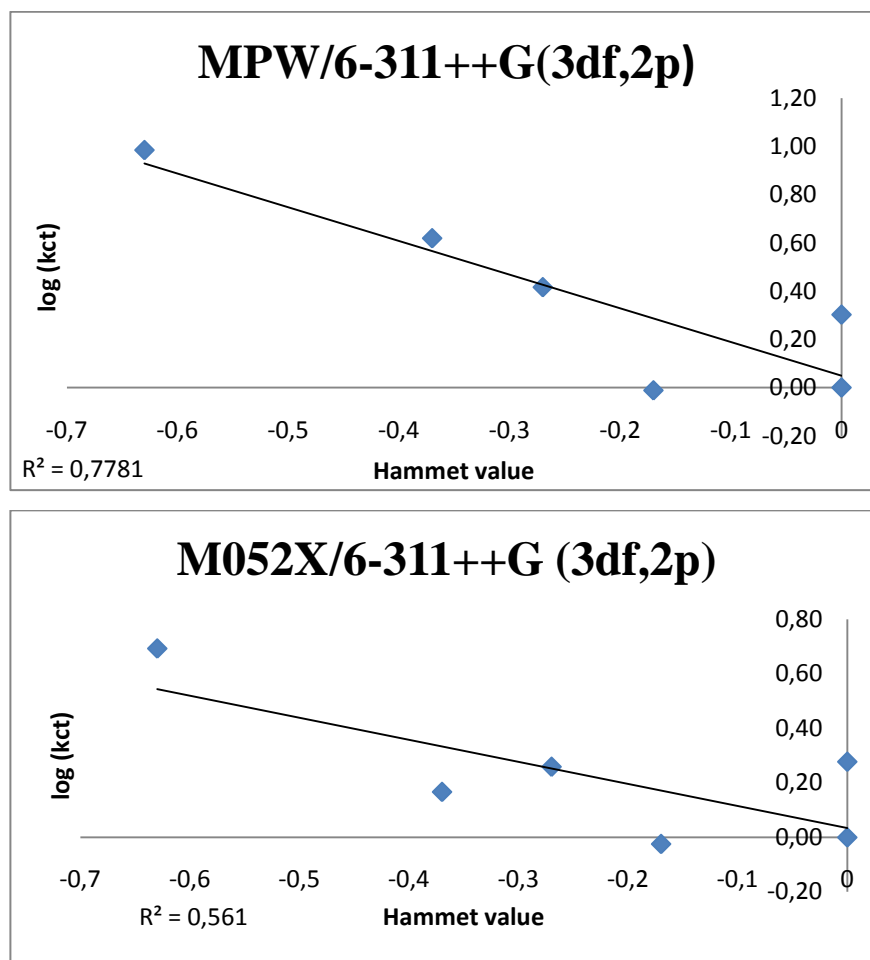
Figure 5.14. Hammet values vs k_{ct} continued

The thiophenols with weak electron donor substituents deviate significantly from linearity (T1, T3 and T4), R = 0.91 for the experimental results. The rate of chain transfer agents is directly proportional to the electronic strength of the substitiuents.

For calculated results, the best linearity was obtained by B3LYP/6-31+G(d) method with a correlation coefficient R=0.82, the other methods ranked as follows MPWB1K/6-311++G(3df,2p) (R=0.78), B3LYP/6-311++G(3df,2p) (R=0.72) and M05-2X/6-311++G(3df,2p) (R= 0.56). By excluding the molecule T3, the straight line is appropriated with MPWB1K/6-311++G(3df,2p) with R= 0.88.

Chain transfer constants (C_s) are calculated by using equation 5.7. The calculated and experimental results are tabulated in Figure 5.15. The most accurate results for C_s in

magnitude was obtained by using the M05-2X/6-311++G(3df,2p) method. Logarithms of C_s were plotted to investigate the trend of different thiophenols (Table 5.3). The correlation between the calculated trend and experimental trend is discussed. The experimental trend was reproduced best by MPWB1K/6-311++G(3df,2p) method. (Figure 5.15)

Table 5.3. Calculated and experimental Cs results

Substitiuition of thiophenols	Cs exp [1]	Cs Calculated			
		B3LYP*	B3LYP **	MPWB1K	M05-2X
-H	0.29	2.13E+02	1.01E+02	3.84E+00	2.16E+00
$-NHCOCH_3$	0.20	3.25E+02	2.58E+02	8.24E+00	4.37E+00
$-CH_3$	0.27	2.00E+02	9.74E+01	3.74E+00	2.04E+00
$-OCH_3$	0.41	5.76E+02	5.29E+02	1.00E+01	3.92E+00
-OH	0.65	5.10E+02	4.94E+02	1.60E+01	3.17E+00
$-NH_2$	2.70	1.50E+03	1.25E+03	3.71E+01	1.06E+01
* B3LYP/6-31+G(d), ** B3LYP/6-311++G(3df,2p)					
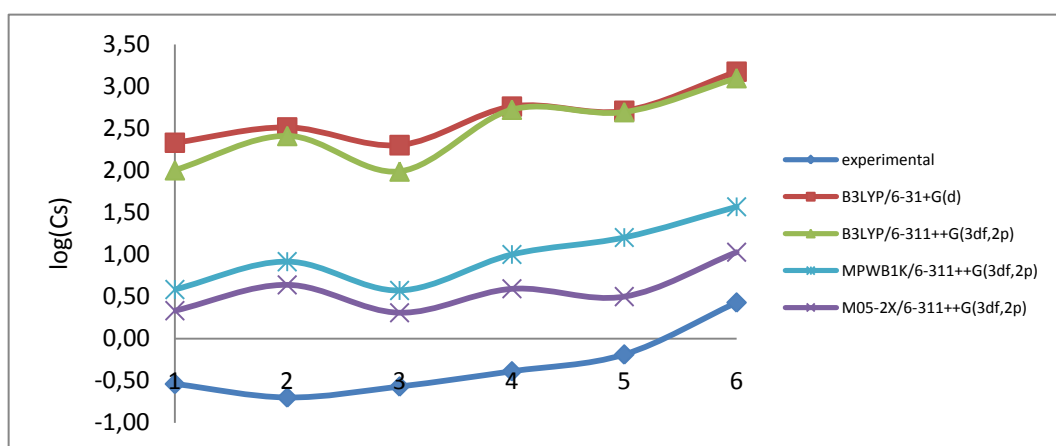
Figure 5.15. log (Cs) vs chain transfer agents.

5.4 Conclusions

In this study the reactions taking place along the polymerization of acrylamide in the presence of a series of thiophenol molecules (T1-T6) have been modeled and discussed.

Propagation rate analysis showed that most accurate results can be obtained by using M05-2X/6-311++G(3df,2p) method. The highest rate constant was obtained with the molecule T6 which bears the strong electron donor NH_2 group. The rate of chain transfer agents is directly proportional to the electronic features of the substitiuents. The correlation between the calculated trend of the chain transfer constants and the experimental results can be best reproduced with the MPWB1K/6-311++G(3df,2p) methodology.

REFERENCES

1. Billmeyer F. W., *Textbook of Polymer Science,* Willey-Interscience Publication, Singapore, 1984.

2. Butler G., *Cyclopolymerization and Cyclocopolymerization*, Marcel Dekker, New York, 1992.

3. Robello, D. R., *Introduction to Polymer Chemistry*, http.//www.chem.rochester.edu /~chem421/frpolym.htm, 2002.

4. Beuermann, S. and M. Buback, "Rate Coefficients of Free Radical Polymerization Deduced from Pulsed Laser Experiments", *Prog. Polym. Sci.*, Vol. 27, pp. 191-254, 2002.

5. Fernández-Garcia, M., M. Fernández-Sanz and E. L. Madruga, "A Kinetic Study of Butyl Acrylate Free Radical Polymerization in Benzene Solution", *Macromol. Chem. Phys.*, Vol. 201, pp. 1840-1845, 2000.

6. Parr, R. G. and W. Yang, *Density Functional Theory of Atoms and Molecules*, Oxford University Press, New York, 1989.

7. Becke, A. D., "Density Functional Exchange Energy Approximation with Correct Asymptotic Behaviour", Vol. 2, pp. 91-123, 1994.

8. Becke, A. D., "A New Mixing of Hartree-Fock and Local Density Functional Theories", *J. Chem. Phys.*, Vol. 38, pp. 1372-1377, 1993.

9. Handy, N. C., "Density Functional Theory", Vol. 2, pp. 91-123, 1994.

10. Leach, A. R., *Molecular Modelling Principles and Applications*, Prentice Hall, England, 2001.

11. Becke, A. D., "Density-Functional Exchange Energy Approximation with Correct Asymptotic Behavior", *Phys. Rev. A*., Vol. 38, pp. 3098-3103, 1988.

12. Becke, A. D., "A New Mixing of Hartree-Fock and Local Density Functional Theories", *J. Chem. Phys*., Vol. 38, pp. 1372-1377, 1993.

13. Lee, C., W. Yang and R. G. Parr, "Development of Colle-Salvatti Correlation Energy Formula into a Functional of the Electron Density", *Phys. Rev. B*, Vol. 37, pp. 785-789, 1988.

14. Becke, A. D., "Density Functional Thermochemistry. III. The Role of Exact Exchange", *J. Chem. Phys*., Vol. 98, pp. 5648-5652, 1993.

15. Pauling, L. J., "The Nature of the Chemical Bond. IV. The Energy of Single Bonds and the Relative Electronegativity of Atoms", *J. Am. Chem. Soc*., Vol. 54, pp. 3570-3582, 1932.

16. Pearson, R. G., "Maximum Chemical and Physical Hardness", *J. Chem. Ed*., Vol. 76, pp. 267-275, 1999.

17. Roy, R. K., S. Krishnamurti, P. Geerlings, and S. Pal, "Local Softness and Hardness Based Reactivity Descriptors for Predicting Intra- and Intermolecular Reactivity Sequences. Carbonyl Compounds", *J. Phys. Chem. A*, Vol. 102, pp. 3740-3755, 1998.

18. Geerlings, P. and F. D. Proft, "HSAB Principle. Applications of Its Global and Local Forms in Organic Chemistry", *Int. J. Quantum Chem*., Vol. 80, pp. 227-235, 2000.

19. Parr, R. G., and W. T. Yang, "Density Functional-Approach to the Frontier-Electron Theory of Chemical-Reactivity", *J. Am. Chem. Soc.*, Vol. 106, pp. 4049-4050, 1984

20. Tomasi, J., Mennucci, B. and E.J. Cancès, "The IEF version of the PCM solvationmethod. an overview of a new method addressed to study molecular solutes at the QM ab initio level ", *Mol. Struct. (THEOCHEM)*, Vol. 464, pp. 211-226, 1999.

21. Tomasi, J., Benedetta, M. and R. Cammi, "Quantum Mechanical Continuum Solvation Models", *Chem. Rev.*, Vol. 105, pp. 2999-3093, 2005.

22. Zubov, V. P., Kumar, M. V., Masterova, M. N., and V. Kabanov,. *Macromol. Sci-Chem.* Vol. 13, pp.111, 1979.

23. Matsumoto, A., "Polymerisation of Multiallyl Monomers", *Prog. Polym. Sci.*, Vol. *26*, pp. 189-257, 2001.

24. Harada, S., and S. Hasegawa, "Homopolymerization of monoallylammonium salts with azo-initiators", *Macromol. Chem. Rapid Commun.*, Vol. 5, pp. 27, 1984.

25. Butler, G. B., and R. L. Bunch, "Preparation and Polymerization of Unsaturated Quaternary Ammonium Compounds", *J. Am. Chem. Soc.*, Vol. 71, pp. 3120, 1949.

26. Butler, G. B., and F. L. Ingley, "Preparation and Polymerization of Unsaturated Quaternary Ammonium Compounds. II. Halogenated Allyl Derivatives", *J. Am. Chem. Soc.*, Vol. 73, pp. 894, 1951.

27. Wandrey C., J.H. Barajas, and D. Hunkeler, "Diallyldimethylammonium Chloride and Its Polymers", *Adv. Polym. Sci.*, Vol. 145, pp. 125-177, 1999.

28. Tüzün, N. S., and V. Aviyente, "A Computational Study on the Substituent Effect of Diallylamine Monomers in Their Cyclopolymerization Reactions", *J. Phys. Chem. A*, Vol. 106, pp. 8184-8190, 2002.

29. Tüzün, N. S. and V. Aviyente, "Modeling the Cyclopolymerization of Diallyl Ether and Methyl α-[(allyloxy)Methyl]acrylate", *Int. J. Quantum Chem.*, Vol. 107, pp. 894-906, 2007.

30. Tüzün, N. S., Aviyente, V., and K. N. Houk, "A Theoretical Study on the Mechanism of the Cyclopolymerization of Diallyl Monomers" *J. Org. Chem.*, Vol. 68, pp. 6369-6374, 2003.

31. Tüzün, N. S., Aviyente, V., and K. N. Houk, "Theoretical Study of Factors Controlling Rates of Cyclization of Radical Intermediates from Diallylamine and Diallylammonium Monomers in Radical Polymerizations", *J. Org. Chem.*, Vol. 67, pp. 5068-5075, 2002.

32. Pinter, B., De Proft, F., Van Speybroeck, V., Hemelsoet, K., Waroquier, M., Chamorro, E., Veszpremi, T., and P. Geerlings, " Spin-polarized Conceptual Density Functional Theory Study of the Regioselectivity in Ring Closures of Radicals", *J. Org. Chem.*, Vol. 72, pp. 348-356, 2007.

33. Kodaira, T., Liu, Q.-Q., Satoyama, M., Urushisaki, M., and H. Utsumi, H. "Cyclopolymerization. XXVI. Repeating Unit Structure of Cyclopolymers Derived from N-substituted-N-allyl-2-(methoxycarbonyl)allylamines and Mechanism of Intramolecular Cyclization", *Polymer*, Vol. 40, pp. 6947-6954, 1999.

34. Pinter, B.; De Proft, F.; Van Speybroeck, V.; Hemelsoet, K.; Waroquier, M.; Chamorro, E.; Veszpremi, T.; Geerlings, P. "Spin-polarized conceptual DFT study of the regioselectivity in ring closures of radicals", *Journal of Organic Chemistry* 2007, *72*, 348-356.

35. Kodaira T., Fujisavva T., Liu Q-Q., and M. Urushisaki, "Cyclopolymerization. 22. Radical Polymerization of N-Methyl-N-allyl-2-(methoxtcarbonyl)allylamine. Design of Unconjugated Dienes with High Polymerizability and High Cyclization Tendency Using Functional Groups of Low Polymerizabilities", *Macromolecules*, Vol. 29, pp. 484-485, 1996.

36. For a detailed account on these types of basis sets, see, e.g., Hehre, W. J.; Radom, L.; Schleyer, P. v. R, and J.A. Pople, *Ab Initio Molecular Orbital Theory*, Wiley, New York, 1986.

37. Gaussian 03, Revision B.05, Frisch, M. J., Gaussian, Inc., Wallingford CT, 2004.

38. Reed, A. E., Weinstock, R. B., and F. Weinhold, "Natural Population Analysis", *J. Chem. Phys.*, Vol. 83, pp. 735, 1985.

39. Reed, A. E., and F. Weinhold, "Natural localized molecular orbitals", *J. Chem. Phys.*, Vol. 83, pp. 1736, 1985.

40. Reed, A. E., Curtiss, L. A., and F. Weinhold, "Intermolecular Interactions from a Natural Bond Orbital, Donor-Acceptor Viewpoint", *Chem. Rev.*, Vol. 88, pp. 899, 1988.

41. Tomasi, J., Mennucci, B., and E. Cancès, "The ief version of the PCM solvation method. An overview of a new method addressed to study molecular solutes at the QM ab initio level", *J. Mol. Struct. (THEOCHEM)*, Vol. 464, pp. 211-226, 1999.

42. Cancès, M. T., Mennucci, B., and J. Tomasi, "A new integral equation formalism for the polarizable continuum model: Theoretical background and applications to isotropic and anisotropic dielectrics", *J. Chem. Phys.*, Vol. 107, pp. 3032-3041, 1997.

43. Mennucci, B., and J. Tomasi, "Derivatives with respect to nuclear coordinates", *J. Chem. Phys.*, Vol. 106, pp. 5151-5158, 1997.

44. Mennucci, B., Cancès, E., Tomasi, J., "Continuum solvation models. A new approach to the problem of solute's charge distribution and cavity boundaries", *J. Phys. Chem. B*, Vol. 101, pp. 10506-10517, 1997.

45. Parr, R. G., and W. Yang, "New measures Of aromaticity - absolute hardness and relative hardness", *J. Am. Chem. Soc*., Vol. 111, pp. 7371-7379, 1989.

46. Parr, R. G., and W. Yang, "Density functional theory of the electronic structure of molecules", *Ann. Rev. Phys. Chem*., Vol. 46, pp. 701, 1995.

47. Kohn, W., Parr, R. G., and A.D. Becke, "Density functional theory of electronic structure", *J. Phys. Chem.*, Vol. 100, pp. 12974- 12980, 1996.

48. W. Langenaeker, Geerlings, P., and F. De Proft, "Ab initio and density functional theory study of the geometry and reactivity of benzyne, 3-fluorobenzyne, 4-fluorobenzyne, and 4,5-didehydropyrimidine", *J. Phys. Chem. A*, Vol. 102, pp. 303, 1998.

49. Chermette, H. "Chemical Reactivity Indexes in Density Functional Theory" *J. Comput. Chem.*, Vol. 20, pp. 129, 1999.

50. Geerlings, P., De Proft, F., and W. Langenaeker, "Conceptual Density Functional Theory", *Chem. Rev.*, Vol. 103, pp. 1793, 2003.

51. Ayers, P. W. , Anderson, J. S. M., and L.J. Bartolotti, "Perturbative Perspectives on the Chemical Reaction Prediction Problem", *Int. J. Quantum Chem.*, Vol. 101, pp. 520, 2005.

52. Liu, S. B. *Acta Phys. Chim. Sin.*, Vol. 25, 2009, in press.

53. Parr, R. G., and W. T. Yang, "Density functional approach to the frontier-electron theory of chemical reactivity", *J. Am. Chem. Soc.*, Vol. 106, pp. 4049, 1984.

54. Ayers, P. W., and M. Levy, "Perspective on density functional approach to the frontier-electron theory of chemical reactivity", *Theor. Chem. Acc.*, Vol. 103, pp. 353, 2000.

55. Perdew, J. P., Parr, R. G., Levy, M. , and J. L. Balduz, "Density-functional theory for fractional particle number: Derivative discontinuities of the energy", *Phys. Rev. Lett.*, Vol. 49, pp. 1691, 1982.

56. Ayers, P. W., "The continuity of the energy and other molecular properties with respect to the number of electrons", *J. Math. Chem.*, Vol. 43. pp. 285-303, 2008.

57. Morell, C., Grand, A., and A. Toro-Labbe, "New dual descriptor for chemical reactivity", *J. Phys. Chem. A.,* Vol. 109, pp. 205, 2005.

58. Ayers, P. W., Morell, C., De Proft, F., and P. Geerlings, "Understanding the Woodward-Hoffmann rules by using changes in electron density", *Chem. Eur. J.*, Vol. 13, pp. 8240, 2007.

59. Parr, R. G., Von Szentpaly, L., and S.B. Liu, "Electrophilicity index" *J. Am. Chem. Soc.*, Vol. 121, pp. 1922, 1999.

60. Chattaraj, P. K., Sarkar, U., and D.R. Roy, "Electrophilicity index" *Chem. Rev.*, Vol. 106, pp. 2065, 2006.

61. Parr, R. G., Donnelly, R. A., Levy, M., and W.E. Palke, "Electronegativity- The density functional viewpoint" *J. Chem. Phys.*, Vol. 68, pp. 3801, 1978.

62. Parr, R. G., and R.G. Pearson, "Absolute hardness: comparrion parameter to absolute electronegativity" *J. Am. Chem. Soc.*, Vol. 105, pp. 7512, 1983.

63. Pearson, R. G., *Chemical Hardness*, Wiley-VCH Weinheim, Germany, 1997.

64. Ayers, P. W., "The physical basis of the global and local hard/soft acid/base principles", *Faraday Discuss.*, Vol 135, pp. 161, 2007.

65. Galvan, M., Vela, A., and J. L. Gazquez, "Chemical reactivity in spin-polarized density functional theory", *J. Phys. Chem.*, Vol. 92, pp. 6470, 1988.

66. Pérez, P., Chamorro, E., and P. W. Ayers, "Representation of spin polarized density functional theory", *J. Chem. Phys.*, Vol. 124, pp. 204108, 2008.

67. Ghanty, T. K., and S. K. Ghosh, "A frontier orbital densityfunctional approach to polarizability, hardness, electronegaitvity, and covalent radius of atomic systems." *J. Am. Chem. Soc.*, Vol. 116, pp. 3943, 1994.

68. Garza, J., Vargas, R., Cedillo, A., Galvan, M., and P. K. Chattaraj, "Reactivity criteria in spin-polarized density functional theory", *Theor. Chem. Acc.* , Vol. 115, pp. 257, 2006.

69. Chamorro, E., Pérez, P., Duque, M., De Proft, F., and P. Geerlings, "Dual descriptors within the framework of spin-polarized density functional theory", *J. Chem. Phys.* , Vol. 129, pp. 064117, 2008.

70. Kodaira, T., Kasajima, N., and M. Urushisaki, "Cyclopolymerization. Part XXVII. Cyclopolymerizability of an unconjugated diene with functional groups with no homopolymerization tendency: radical polymerization of *N*-methyl-*N*-methallyl-2-(methoxycarbonyl)allylamine and structure of the polymers derived therefrom", *Polymer*, Vol.41, pp. 2831-2837, 2000.

71. Johns, S. R., and R. I. Willing, *J.* "Cyclopolymerization of diallylamides and diallylsulphonamides", *Macromol. Sci.sChem. A.* , Vol. 10, pp. 875-891,1976.

72. Butler, GB, *Cyclopolymerization and Cyclocopolymerization*, Marcel Dekker, Inc., New York, pp. 54, 1992.

73. Butler, GB, *Cyclopolymerization and Cyclocopolymerization*, Marcel Dekker, Inc., New York, pp. 71, 1992.

74. Butler, GB, *Cyclopolymerization and Cyclocopolymerization*, Marcel Dekker, Inc., New York, pp.257, 1992.

75. Morton, M., and L. J. Fetters, "Homogeneous Anionic Polymerization of Unsaturated Monomers", *Journal of Polymer Science*, Vol:2, pp. 71-113, 1967.

76. Beckwith, A. L. J., "Regio-Selectivity and stereo-selectivity ın radical reactions", *Tetrahedron*, Vol. 37, pp. 3073-3075, *1981*.

77. Capon, B., Rees, C. W., *Annu. Rep. Chem. Soc.*, Vol. 61, pp 221, 1964.

78. De Vleeschouwer, F., Van Speybroeck, V., Waroquier, M., Geerlings, P., and F. De Proft, "Electrophilicity and nucleophilicity index for radicals", *Org. Lett.*, Vol.9, pp.2721, 2007.

79. Matyjaszewski K, and T. Davis, *Radical Polymerization*, John Wiley and Sons, Canada, 1998.

80. Chang Q, Hao X., and L. Duan, "Synthesis of crosslinked starch-graft-polyacrylamide-*co*-sodium xanthate and its performances in wastewater treatment", *J. Haz. Materials*, Vol.159, pp. 548, 2008.

81. Sojka R., Bjorneberg D., and J.A. Entry, et al., "Polyacrylamide in agriculture and environmental land management", *Adv. In Agronomy*, Vol. 92, pp. 75, 2007.

82. Patrick T., "Polyacrylamide gel in cosmetic procedures: Experience with AQUAMID", *Sem. Cut. Medicine and Surgery*, Vol.23, pp. 233-235, 2004.

83. Ravindra S, Mohan YM, and K. Varaprasad, et al., "Surfactant-Modified Poly(acrylamide-co-acrylamido propane sulphonic acid) Hydrogels, *International Journal Of Polymeric Materials*, Vol. 58, pp. 278- 296, 2009.

84. Ehrbar M., Schoenmakers R., and E. Christen, et al., "Drug-sensing hydrogels for the inducible release of biopharmaceuticals", *Nature Materials*, Vol.7, pp. 800-804, 2008.

85. Valdebenito A., and M.V. Encinas, "Thiophenols as chain transfer agents in the polymerization of vinyl monomers", *Polymer,* Vol. 46, pp. 10658-10662, 2005.

86. Moad G, and D.H. Solomon, *The Chemistry Of Free Radical Polymerization*, Oxford Pergamon Press, London, 1995.

87. Zhao R., Lind J., Merenyi G., and T.E. Eriksen, "Kinetics Of One-Electron Oxidation Of Thiols And Hydrogen Abstraction By Thiyl Radicals From Alpha-Amino C-H Bonds" *J Am Chem Soc*, Vol. 116, pp. 12010-12015, 1994.

88. Zhao Y., Gonza´lez-Garcı´a N., and D. Truhlar., "Benchmark database of barrier heights for heavy atom transfer, nucleophilic substitution, association, and unimolecular reactions and their use to test DFT", *J. Phys. Chem. A*, Vol. 109, pp. 2912-2018, 2005.

89. Zhao Y., Schultz N., and D. Truhlar., "Assessment of model chemistry methods for noncovalent interactions", *J. Chem. Theory Comput.* , Vol. 2, pp. 364-382, 2006.

90. Zhao, Y., and D. G. Truhlar, "Development and assessment of a new hybrid density functional method for thermochemical kinetics", *J. Phys. Chem. A.* , Vol.108, pp. 6908-6918, 2004.

91. Atkins P., and J. Paulo, *Physical Chemistry*, Oxford University Press, New York, 2002.

92. Değirmenci, İ., Avcı, D., Aviyente, V., Van Cauter, K., Van Speybroeck, V., and M. Waroquier, "A DFT Study of Free-Radical Polymerization of Acrylates: Structure-Reactivity Relationship", *Macromolecules*.,Vol. 40, pp. 9590-9602, 2007.

93. Değirmenci, İ., Aviyente, V., Van Speybroeck, V., and M. Waroquier, "DFT Study on the Propagation Kinetics of Free-Radical Polymerization of alpha-Substituted Acrylates", *Macromolecules,* Vol. 42, pp. 3033-3041, 2009.

94. Hammett L.P., *Physical Organic Chemistry*, McGraw-Hill, New York, 1940.